Supplementary Information

Bacterial adaptation through distributed sensing of metabolic fluxes

Oliver Kotte, Judith B. Zaugg & Matthias Heinemann

Contents

---

1 Model structure

This section presents in detail the mechanistic model of *E. coli*'s central carbon metabolism and its regulation discussed in the main paper.

1.1 Strategy for the derivation of the model topology

The topology of the model is shown in Figure 1 of the main paper. This topology comprises two compartments. The first compartment represents the cells' closed environment (as in batch experiments). The environment contains a population of identical cells and the two carbon sources glucose and acetate. The second compartment represents the cells.

The topology of the cellular compartment is centered on the five known transcription factor (TF)-metabolite interactions in *E. coli*'s central metabolism (Cra-fructose-1,6-bisphosphate, Crp-cyclic AMP, IclR-glyoxylate, IclR-pyruvate, and PdhR-pyruvate). The topology was derived with the following strategy:

1. The topology is seeded with the five TF-metabolite-interactions and the two carbon sources glucose and acetate.

2. The seeded metabolites are connected to each other through the inclusion of metabolic pathways.

3. The enzymes catalyzing the metabolic reactions are added. In the case of isozymes, only the dominant enzyme is chosen.

4. Regulations of enzyme activity through metabolites appearing in the model, and through phosphorylations, are added.

5. The expression of the modeled enzymes is added, along with their known transcriptional regulations by the four TFs. The concentrations of the TFs themselves and of the phosphotransferase system (PTS) proteins are modeled as constant. The intermediate mRNA is ignored.

6. The model is simplified by merging linear pathways to single reactions whenever the eliminated metabolic intermediates do not appear as effectors elsewhere in the model, and the merged enzymes are unregulated or co-regulated by the same TF.

7. The production of biomass from the precursor metabolites and the calculation of the growth rate are added.

1.2 Overview of the model structure

When translated into mathematical equations, the model comprises 47 state variables $\mathbf{x}$, 193 parameters $\mathbf{p}$, and 109 rate equations $\mathbf{f}(\mathbf{x}, \mathbf{p})$. Given an initial condition $\mathbf{x}(t = 0)$, the progression of the state variables over the independent variable, the time t, is given by $\dot{\mathbf{x}} = \mathbf{S} \cdot \mathbf{f}(\mathbf{x}, \mathbf{p})$, with $\mathbf{S}$ the constant stoichiometric matrix of dimension 47 x 109. Hence, $\mathbf{S} \cdot \mathbf{f}$ calculates the differential change of the state variables from the rates occurring in the system. The model is thus fully described by ($\mathbf{x}$, $\mathbf{p}$, $\mathbf{f}$, $\mathbf{S}$).

The 47 state variables, arranged in the vector $\mathbf{x}$, are shown in Table S3. This table lists the full names of the molecular compounds represented by the 47 state variables x_{abbrv}, with $_{abbrv}$ the abbreviations for the represented compounds. Table S3 also lists the measured or derived values during balanced growth on glucose and acetate, which were used for parameter estimation (see Section 2 of this Supplementary Information) and as initial conditions for the simulations reported in the main paper.

The 109 rates, arranged in the vector $\mathbf{f}$, are shown in Table S4. This table lists the full names of the molecular rates represented by the 109 rates f_{abbrv}, with $_{abbrv}$ the abbreviations for the represented rates. Table S4 also lists the measured or derived values during balanced growth on glucose and acetate, which are used for parameter estimation (see Section 2 of this Supplementary Information).

The 193 parameters, which appear in the rate equations $\mathbf{f}(\mathbf{x}, \mathbf{p})$, are arranged in the vector $\mathbf{p}$ and shown in Table S5. This table lists the mechanistic meaning of the parameters and their estimated values (see Section 2).

The stoichiometric matrix $\mathbf{S}$ is mostly zero, except at few entries. Rather than presenting this sparse 47 x 109 matrix directly, it is far more informative to present the 47 equations that arise when $\mathbf{S} \cdot \mathbf{f}$ is multiplied out (see next Section). If needed, the stoichiometric matrix $\mathbf{S}$ can be deduced from these equations, or extracted from the MATLAB source code.

1.3 Balance equations

The 47 differential equations, which describe the time progression of the 47 state variables over time as a function of the system's rates, balance the

- biomass of the cell population
- concentrations of extracellular carbon sources
- concentrations of metabolites
- concentrations and phosphorylation states of enzymes and PTS proteins
- binding states of transcription factors.

The balance equations are:

Biomass

$$\dot{x}_{OD} = f_{ENV,growth}$$

Extracellular carbon sources

$$\dot{x}_{ACT} = f_{ENV,ACTex} - f_{ENV,ACTup}$$
$$\dot{x}_{GLC} = -f_{ENV,GLCup}$$

Metabolites

$$\dot{x}_{ACoA} = f_{E,Acs} + f_{E,Pdh} - f_{E,Acoa2act} - f_{E,GltA} - f_{E,AceB} - f_{D,ACoA} - f_{BM,ACoA}$$
$$\dot{x}_{AKG} = f_{E,AceA} + f_{E,Icd} - f_{E,Akg2mal} - f_{D,AKG} - f_{BM,AKG}$$
$$\dot{x}_{cAMP} = f_{E,Cya} - f_{E,CAMPdegr} - f_{D,cAMP}$$
$$\dot{x}_{FBP} = f_{E,PfkA} - 0.5 \cdot f_{E,Emp} - f_{E,Fdp} - f_{D,FBP}$$
$$\dot{x}_{G6P} = f_{E,Fdp} - f_{E,PfkA} + f_{PTS,r_4} - f_{D,G6P} - f_{BM,G6P}$$
$$\dot{x}_{GLX} = f_{E,AceA} - f_{E,AceB} - f_{D,GLX}$$
$$\dot{x}_{ICT} = f_{E,GltA} - f_{E,AceA} - f_{E,Icd} - f_{D,ICT}$$
$$\dot{x}_{MAL} = f_{E,AceB} + f_{E,Akg2mal} - f_{E,MaeAB} - f_{E,Mdh} - f_{D,MAL}$$
$$\dot{x}_{OAA} = f_{E,Ppc} + f_{E,Mdh} - f_{E,PckA} - f_{E,GltA} - f_{D,OAA} - f_{BM,OAA}$$
$$\dot{x}_{PEP} = f_{E,PckA} + f_{E,PpsA} + f_{E,Eno} - f_{E,Ppc} - f_{E,PykF} - f_{PTS,r_1} - f_{D,PEP} \cdots - f_{BM,PEP}$$
$$\dot{x}_{PG3} = f_{E,Emp} - f_{E,Eno} - f_{D,PG3} - f_{BM,PG3}$$
$$\dot{x}_{PYR} = f_{E,MaeAB} + f_{E,PykF} - f_{E,Pdh} - f_{E,PpsA} + f_{PTS,r_1} - f_{D,PYR} - f_{BM,PYR}$$

Enzymes and PTS proteins

$$\dot{x}_{AceA} = f_{G,aceA} - f_{D,AceA}$$
$$\dot{x}_{AceB} = f_{G,aceB} - f_{D,AceB}$$
$$\dot{x}_{AceK} = f_{G,aceK} - f_{D,AceK}$$
$$\dot{x}_{Acoa2act} = f_{G,acoa2act} - f_{D,Acoa2act}$$
$$\dot{x}_{Acs} = f_{G,acs} - f_{D,Acs}$$
$$\dot{x}_{Akg2mal} = f_{G,akg2mal} - f_{D,Akg2mal}$$
$$\dot{x}_{CAMPdegr} = f_{G,campdegr} - f_{D,CAMPdegr}$$
$$\dot{x}_{Cya} = f_{G,cya} - f_{D,Cya}$$
$$\dot{x}_{Emp} = f_{G,emp} - f_{D,Emp}$$
$$\dot{x}_{Eno} = f_{G,eno} - f_{D,Eno}$$
$$\dot{x}_{Fdp} = f_{G,fdp} - f_{D,Fdp}$$
$$\dot{x}_{GltA} = f_{G,gltA} - f_{D,GltA}$$

$$
\begin{aligned}
\dot{x}_{Icd} &= f_{G,icd} - f_{D,Icd} - f_{E,AceK-Ki} + f_{E,AceK-Ph} \\
\dot{x}_{Icd-P} &= -f_{D,Icd-P} + f_{E,AceK-Ki} - f_{E,AceK-Ph} \\
\dot{x}_{Mdh} &= f_{G,mdh} - f_{D,Mdh} \\
\dot{x}_{MaeAB} &= f_{G,maeAB} - f_{D,MaeAB} \\
\dot{x}_{PckA} &= f_{G,pckA} - f_{D,PckA} \\
\dot{x}_{Pdh} &= f_{G,pdh} - f_{D,Pdh} \\
\dot{x}_{PfkA} &= f_{G,pfkA} - f_{D,PfkA} \\
\dot{x}_{Ppc} &= f_{G,ppc} - f_{D,Ppc} \\
\dot{x}_{PpsA} &= f_{G,ppsA} - f_{D,PpsA} \\
\dot{x}_{PykF} &= f_{G,pykF} - f_{D,PykF} \\
\dot{x}_{EIIA} &= f_{G,eiia} - f_{D,EIIA} - f_{PTS,r_1} + f_{PTS,r_4} \\
\dot{x}_{EIIA-P} &= -f_{D,EIIA-P} + f_{PTS,r_1} - f_{PTS,r_4} \\
\dot{x}_{EIICB} &= f_{G,eiicb} - f_{D,EIICB}
\end{aligned}
$$

Transcription factors

$$
\begin{aligned}
\dot{x}_{Cra} &= f_{G,cra} - f_{D,Cra} - f_{TF,Cra} \\
\dot{x}_{CraFBP} &= -f_{D,CraFBP} + f_{TF,Cra} \\
\dot{x}_{Crp} &= f_{G,crp} - f_{D,Crp} - f_{TF,Crp} \\
\dot{x}_{CrpcAMP} &= -f_{D,CrpcAMP} + f_{TF,Crp} \\
\dot{x}_{IclR} &= f_{G,iclR} - f_{D,IclR} \\
\dot{x}_{PdhR} &= f_{G,pdhR} - f_{D,PdhR} - f_{TF,PdhR} \\
\dot{x}_{PdhRPYR} &= -f_{D,PdhRPYR} + f_{TF,PdhR}
\end{aligned}
$$

The 109 individual rates $f(\mathbf{x}, \mathbf{p})$ that appear in these differential equations are structured in the six units

1. Cell growth and carbon source dynamics
2. Metabolic reactions and protein phosphorylations
3. Transcription factor- metabolite bindings
4. Gene expression
5. Dilution and degradation of compounds
6. Biomass generation and growth rate calculation.

The following six sections describe in detail the modeling of these units and present the mechanistic rate equations $\mathbf{f}(\mathbf{x}, \mathbf{p})$ belonging to these units.

1.4 Cell growth and carbon source dynamics

The closed environment is fully described by the extracellular concentrations of the two carbon sources glucose (x_{GLC}) and acetate (x_{ACT}), both of the unit $g\,l^{-1}$. The size of the *E. coli* cell population within this environment is given by its biomass concentration (x_{OD}).

To model the interaction of the *E. coli* cells with their environment, the substrate exchange rates between the two compartments need to be quantified. Rates in the compartment containing the intracellular processes are normalized to cell dry weight and are of the unit $\mu mol\,(g_{DW}\,s)^{-1}$; rates in the compartment containing the environment scale with the biomass concentration of the cell population and are of the unit $g_{SUBSTRATE}\,(l \cdot s)^{-1}$. Therefore, to quantify the substrate exchange rates of the whole cell population, the substrate exchange rates of dry weight-normalized cells, calculated in Section 1.5, need to be scaled with the biomass concentration and converted to the proper units. The parameters needed to quantify this conversion are the molar mass of glucose $p_{ENV,M_{GLC}}$, the molar mass of acetate $p_{ENV,M_{ACT}}$, and the remaining unit conversions subsumed in $p_{ENV,UC}$.

The rate equations describing cell growth and the production and consumption of environmental carbon sources are:

$$
\begin{aligned}
f_{ENV,growth} &= \mu\, x_{OD} \\
f_{ENV,GLCup} &= p_{ENV,M_{GLC}}\, p_{ENV,UC}\, x_{OD}\, f_{PTS,r4} \\
f_{ENV,ACTup} &= p_{ENV,M_{ACT}}\, p_{ENV,UC}\, x_{OD}\, f_{E,Acs} \\
f_{ENV,ACTex} &= p_{ENV,M_{ACT}}\, p_{ENV,UC}\, x_{OD}\, f_{E,Acoa2act}
\end{aligned}
$$

1.5 Metabolic reactions and protein phosphorylations

All metabolic reactions occurring in the model are catalyzed by enzymes. Also, the phosphorylation and dephosphorylation of the enzyme Icd is catalyzed by the two enzymatic reactions of the enzyme AceK. Further, the uptake and phosphorylation of glucose is achieved with the help of protein phosphorylations occurring in the phosphotransferase system (PTS).

Many of the modeled enzymes are *in vivo* present as multimers and as such most likely exhibit cooperative binding kinetics. We assigned Monod-Wyman-Changeux kinetics to these enzymes. This type of rate law includes the (known) number of a multimer's subunits as a parameter to account for cooperative binding effects. Further, the basic formulation of this rate law can be easily extended to incorporate the effect of multiple activators and inhibitors on the catalyzed reaction rate, which is an important property given the dense enzymatic regulation present in the model. If a multimeric enzyme is not subject to enzymatic regulation, we used a Hill–type kinetics instead to reduce the number of uncertain parameters. We used Michaelis-Menten type rate laws to model the kinetics of monomeric enzymes.

Table S1 lists the chosen types of kinetic equations describing these reactions. The full equations follow this table. The metabolic reactions that produce biomass from the seven modeled precursor metabolites are presented in Section 1.9.

Table S1: Overview of the chosen types of kinetic rate equations for the metabolic reactions and protein phosphorylation processes. The following abbreviations are used: MM – Michaelis-Menten kinetics, revMM – reversible Michaelis-Menten kinetics, 2S-MM – Two-substrate Michaelis-Menten kinetics, MWC – Monod-Wyman-Changeux kinetics, rev2S-1st – Reversible two-substrate first order kinetics, (A) – Activator, (I) – Inhibitor.

Rate	Type	Substrate(s)	Effectors
$f_{E,AceA}$	MWC	ICT	AKG (I), PEP (I), PG3 (I)
$f_{E,AceB}$	2S-MM	GLX, ACoA	—
$f_{E,AceK-Ki}$	MWC	Icd	AKG (I), GLX (I), ICT (I), OAA (I), PEP(I), PG3 (I), PYR (I)
$f_{E,AceK-Ph}$	MWC	Icd-P	AKG (A), OAA (A), PEP (A), PG3 (A), PYR (A)
$f_{E,Acoa2act}$	MWC	ACoA	PYR (A)
$f_{E,Acs}$	MM	ACT	—
$f_{E,Akg2mal}$	MM	AKG	—
$f_{E,CAMPdegr}$	MM	cAMP	—
$f_{E,Cya}$	MM	EIIA-P *	— *
$f_{E,Emp}$	revMM	FBP, PG3	—
$f_{E,Eno}$	revMM	PG3, PEP	—
$f_{E,Fdp}$	MWC	FBP	PEP (A)
$f_{E,GltA}$	2S-MM	ACoA, OAA	AKG (I, competitive)
$f_{E,Icd}$	MWC	ICT	PEP (I)
$f_{E,MaeAB}$	MWC	MAL	ACoA (I), cAMP (I)
$f_{E,Mdh}$	Hill	MAL	—
$f_{E,PckA}$	MM	OAA	PEP (I, competitive)
$f_{E,Pdh}$	MWC	PYR	GLX (I), PYR (I)
$f_{E,PfkA}$	MWC	G6P	PEP (I)
$f_{E,Ppc}$	MWC	PEP	FBP (A)
$f_{E,PpsA}$	MWC	PYR	PEP (I)
$f_{E,PykF}$	MWC	PEP	FBP (A)
f_{PTS,r_1}	rev2S-1st	PEP, EIIA; PYR, EIIA-P	—
f_{PTS,r_4}	MM	EIIA-P, GLC	—

continued on the next page ...

... Table S1 continued.

Rate	Type	Substrate(s)	Effectors

* The Cya reaction is activated by EIIA-P and produces cAMP from void. Because 'void' cannot be a substrate in a mechanistic equation, the Cya reaction is modeled with the activator EIIA-P as substrate. This approach conforms with the one chosen by (Bettenbrock et al, 2006).

$$
\begin{aligned}
f_{E,AceA} = {} & x_{AceA}\, p_{AceA,k_{cat}} \frac{x_{ICT}}{p_{AceA,K_{ICT}}} \Big(1 + \frac{x_{ICT}}{p_{AceA,K_{ICT}}}\Big)^{p_{AceA,n}-1} \dots \\
& \Bigg[\Big(1 + \frac{x_{ICT}}{p_{AceA,K_{ICT}}}\Big)^{p_{AceA,n}} + p_{AceA,L} \Big(1 + \frac{x_{PEP}}{p_{AceA,K_{PEP}}} \dots \\
& + \frac{x_{PG3}}{p_{AceA,K_{PG3}}} + \frac{x_{AKG}}{p_{AceA,K_{AKG}}}\Big)^{p_{AceA,n}} \Bigg]^{-1} \\
f_{E,AceB} = {} & x_{AceB}\, p_{AceB,k_{cat}}\, x_{GLX}\, x_{ACoA} \Big(p_{AceB,K_{GLXACoA}}\, p_{AceB,K_{ACoA}} \dots \\
& + p_{AceB,K_{ACoA}}\, x_{GLX} + p_{AceB,K_{GLX}}\, x_{ACoA} + x_{GLX}\, x_{ACoA} \Big)^{-1} \\
f_{E,AceK-Ki} = {} & x_{AceK}\, p_{AceK,k_{cat,ki}} \frac{x_{Icd}}{p_{AceK,K_{Icd}}} \left(1 + \frac{x_{Icd}}{p_{AceK,K_{Icd}}}\right)^{p_{AceK,n}-1} \dots \\
& \left[\left(1 + \frac{x_{Icd}}{p_{AceK,K_{Icd}}}\right)^{p_{AceK,n}} + p_{AceK,L} \left(1 + \frac{x_{ICT}}{p_{AceK,K_{ICT}}} \dots \right.\right. \\
& + \frac{x_{GLX}}{p_{AceK,K_{GLX}}} + \frac{x_{OAA}}{p_{AceK,K_{OAA}}} + \frac{x_{AKG}}{p_{AceK,K_{AKG}}} + \frac{x_{PEP}}{p_{AceK,K_{PEP}}} \dots \\
& \left.\left. + \frac{x_{PG3}}{p_{AceK,K_{PG3}}} + \frac{x_{PYR}}{p_{AceK,K_{PYR}}}\right)^{p_{AceK,n}} \right]^{-1} \\
f_{E,AceK-Ph} = {} & x_{AceK}\, p_{AceK,k_{cat,ph}} \frac{x_{Icd-P}}{p_{AceK,K_{Icd-P}}} \left(1 + \frac{x_{Icd-P}}{p_{AceK,K_{Icd-P}}}\right)^{p_{AceK,n}-1} \dots \\
& \left[\left(1 + \frac{x_{Icd-P}}{p_{AceK,K_{Icd-P}}}\right)^{p_{AceK,n}} + p_{AceK,L} \left(1 + \frac{x_{OAA}}{p_{AceK,K_{OAA}}} \dots \right.\right. \\
& \left.\left. + \frac{x_{AKG}}{p_{AceK,K_{AKG}}} + \frac{x_{PEP}}{p_{AceK,K_{PEP}}} + \frac{x_{PG3}}{p_{AceK,K_{PG3}}} + \frac{x_{PYR}}{p_{AceK,K_{PYR}}}\right)^{-p_{AceK,n}} \right]^{-1} \\
f_{E,Acoa2act} = {} & x_{Acoa2act}\, p_{Acoa2act,k_{cat}} \frac{x_{ACoA}}{p_{Acoa2act,K_{ACoA}}} \Big(1 + \frac{x_{ACoA}}{p_{Acoa2act,K_{ACoA}}}\Big)^{p_{Acoa2act,n}-1} \dots \\
& \Bigg[\Big(1 + \frac{x_{ACoA}}{p_{Acoa2act,K_{ACoA}}}\Big)^{p_{Acoa2act,n}} \dots
\end{aligned}
$$

$$+ p_{Acoa2act,L}\left(1 + \frac{x_{PYR}}{p_{Acoa2act,K_{PYR}}}\right)^{-p_{Acoa2act,n}}\Bigg]^{-1}$$

$$f_{E,Acs} = \frac{x_{Acs}\, p_{Acs,k_{cat}}\, x_{ACT}}{x_{ACT} + p_{Acs,K_{ACT}}}$$

$$f_{E,Akg2mal} = \frac{x_{Akg2mal}\, p_{Akg2mal,k_{cat}}\, x_{AKG}}{x_{AKG} + p_{Akg2mal,K_{AKG}}}$$

$$f_{E,CAMPdegr} = \frac{p_{CAMPdegr,k_{cat}}\, x_{CAMPdegr}\, x_{cAMP}}{x_{cAMP} + p_{CAMPdegr,K_{cAMP}}}$$

$$f_{E,Cya} = \frac{p_{Cya,k_{cat}}\, x_{Cya}\, x_{EIIA-P}}{x_{EIIA-P} + p_{Cya,K_{EIIA-P}}}$$

$$f_{E,Emp} = \frac{x_{Emp}\left(p_{Emp,k_{cat,f}}\frac{x_{FBP}}{p_{Emp,K_{FBP}}} - p_{Emp,k_{cat,r}}\frac{x_{PG3}}{p_{Emp,K_{PG3}}}\right)}{1 + \frac{x_{FBP}}{p_{Emp,K_{FBP}}} + \frac{x_{PG3}}{p_{Emp,K_{PG3}}}}$$

$$f_{E,Eno} = \frac{x_{Eno}\left(p_{Eno,k_{cat,f}}\frac{x_{PG3}}{p_{Eno,K_{PG3}}} - p_{Eno,k_{cat,r}}\frac{x_{PEP}}{p_{Eno,K_{PEP}}}\right)}{1 + \frac{x_{PG3}}{p_{Eno,K_{PG3}}} + \frac{x_{PEP}}{p_{Eno,K_{PEP}}}}$$

$$f_{E,Fdp} = \frac{x_{Fdp}\, p_{Fdp,k_{cat}}\frac{x_{FBP}}{p_{Fdp,K_{FBP}}}\left(1 + \frac{x_{FBP}}{p_{Fdp,K_{FBP}}}\right)^{p_{Fdp,n}-1}}{\left(1 + \frac{x_{FBP}}{p_{Fdp,K_{FBP}}}\right)^{p_{Fdp,n}} + p_{Fdp,L}\left(1 + \frac{x_{PEP}}{p_{Fdp,K_{PEP}}}\right)^{-p_{Fdp,n}}}$$

$$f_{E,GltA} = x_{GltA}\, p_{GltA,k_{cat}}\, x_{OAA}\, x_{ACoA}\Bigg[\left(1 + \frac{x_{AKG}}{p_{GltA,K_{AKG}}}\right) p_{GltA,K_{OAAACoA}} \cdots$$
$$p_{GltA,K_{ACoA}} + p_{GltA,K_{ACoA}}\, x_{OAA} + \left(1 + \frac{x_{AKG}}{p_{GltA,K_{AKG}}}\right) \cdots$$
$$p_{GltA,K_{OAA}}\, x_{ACoA} + x_{OAA}\, x_{ACoA}\Bigg]^{-1}$$

$$f_{E,Icd} = \frac{x_{Icd}\, p_{Icd,k_{cat}}\frac{x_{ICT}}{p_{Icd,K_{ICT}}}\left(1 + \frac{x_{ICT}}{p_{Icd,K_{ICT}}}\right)^{p_{Icd,n}-1}}{\left(1 + \frac{x_{ICT}}{p_{Icd,K_{ICT}}}\right)^{p_{Icd,n}} + p_{Icd,L}\left(1 + \frac{x_{PEP}}{p_{Icd,K_{PEP}}}\right)^{p_{Icd,n}}}$$

$$f_{E,MaeAB} = x_{MaeAB}\, p_{MaeAB,k_{cat}}\frac{x_{MAL}}{p_{MaeAB,K_{MAL}}}\left(1 + \frac{x_{MAL}}{p_{MaeAB,K_{MAL}}}\right)^{p_{MaeAB,n}-1} \cdots$$
$$\Bigg[\left(1 + \frac{x_{MAL}}{p_{MaeAB,K_{MAL}}}\right)^{p_{MaeAB,n}} + p_{MaeAB,L} \cdots$$
$$\left(1 + \frac{x_{ACoA}}{p_{MaeAB,K_{ACoA}}} + \frac{x_{cAMP}}{p_{MaeAB,K_{cAMP}}}\right)^{p_{MaeAB,n}}\Bigg]^{-1}$$

$$f_{E,Mdh} = \frac{x_{Mdh}\, p_{Mdh,k_{cat}}\, {x_{MAL}}^{p_{Mdh,n}}}{{x_{MAL}}^{p_{Mdh,n}} + p_{Mdh,K_{MAL}}\, {p_{Mdh,n}}}$$

$$f_{E,PckA} = \frac{x_{PckA}\, p_{PckA,k_{cat}}\, x_{OAA}}{x_{OAA} + p_{PckA,K_{OAA}}\left(1 + \frac{x_{PEP}}{p_{PckA,K_{PEP}}}\right)}$$

$$f_{E,Pdh} = \frac{x_{Pdh}\, p_{Pdh,k_{cat}} \frac{x_{PYR}}{p_{Pdh,K_{PYR}}} \left(1 + \frac{x_{PYR}}{p_{Pdh,K_{PYR}}}\right)^{p_{Pdh,n}-1}}{\left(1 + \frac{x_{PYR}}{p_{Pdh,K_{PYR}}}\right)^{p_{Pdh,n}} + p_{Pdh,L}\left(1 + \frac{x_{GLX}}{p_{Pdh,K_{GLX}}} + \frac{x_{PYR}}{p_{Pdh,K_{I,PYR}}}\right)^{p_{Pdh,n}}}$$

$$f_{E,PfkA} = \frac{x_{PfkA}\, p_{PfkA,k_{cat}} \frac{x_{G6P}}{p_{PfkA,K_{G6P}}} \left(1 + \frac{x_{G6P}}{p_{PfkA,K_{G6P}}}\right)^{p_{PfkA,n}-1}}{\left(1 + \frac{x_{G6P}}{p_{PfkA,K_{G6P}}}\right)^{p_{PfkA,n}} + p_{PfkA,L}\left(1 + \frac{x_{PEP}}{p_{PfkA,K_{PEP}}}\right)^{p_{PfkA,n}}}$$

$$f_{E,Ppc} = \frac{x_{Ppc}\, p_{Ppc,k_{cat}} \frac{x_{PEP}}{p_{Ppc,K_{PEP}}} \left(1 + \frac{x_{PEP}}{p_{Ppc,K_{PEP}}}\right)^{p_{Ppc,n}-1}}{\left(1 + \frac{x_{PEP}}{p_{Ppc,K_{PEP}}}\right)^{p_{Ppc,n}} + p_{Ppc,L}\left(1 + \frac{x_{FBP}}{p_{Ppc,K_{FBP}}}\right)^{-p_{Ppc,n}}}$$

$$f_{E,PpsA} = \frac{x_{PpsA}\, p_{PpsA,k_{cat}} \frac{x_{PYR}}{p_{PpsA,K_{PYR}}} \left(1 + \frac{x_{PYR}}{p_{PpsA,K_{PYR}}}\right)^{p_{PpsA,n}-1}}{\left(1 + \frac{x_{PYR}}{p_{PpsA,K_{PYR}}}\right)^{p_{PpsA,n}} + p_{PpsA,L}\left(1 + \frac{x_{PEP}}{p_{PpsA,K_{PEP}}}\right)^{p_{PpsA,n}}}$$

$$f_{E,PykF} = \frac{x_{PykF}\, p_{PykF,k_{cat}} \frac{x_{PEP}}{p_{PykF,K_{PEP}}} \left(1 + \frac{x_{PEP}}{p_{PykF,K_{PEP}}}\right)^{p_{PykF,n}-1}}{\left(1 + \frac{x_{PEP}}{p_{PykF,K_{PEP}}}\right)^{p_{PykF,n}} + p_{PykF,L}\left(1 + \frac{x_{FBP}}{p_{PykF,K_{FBP}}}\right)^{-p_{PykF,n}}}$$

$$f_{PTS,r_1} = p_{PTS,k_1}\, x_{PEP}\, x_{EIIA} - p_{PTS,km_1}\, x_{PYR}\, x_{EIIA-P}$$

$$f_{PTS,r_4} = \frac{p_{PTS,k_4}\, x_{EIICB}\, x_{EIIA_P}\, x_{GLC}}{\left(p_{PTS,K_{EIIA}} + x_{EIIA-P}\right)\left(p_{PTS,K_{GLC}} + x_{GLC}\right)}$$

1.6 Transcription factor–metabolite interactions

The interactions of the transcription factors Cra, Crp and PdhR with the respective metabolites FBP, cAMP, and PYR are modeled with single rate equations each, which combine the association and dissociation rates into one rate. A positive net rate results when the association rate is higher than the dissociation rate, a negative net rate when the reverse is the case. The net rate can be determined by first calculating the association and dissociation rates separately and then joining them to the net rate. This is essentially what the following equation do; however, the calculation of the net rate in these equations is rearranged such that the net rate is determined through scaling (and unit conversion of) the deviation of the actual binding state from the steady state level. The resulting rate equations are:

$$f_{TF,Cra} = p_{Cra,scale}\left[\frac{\left(x_{Cra} + x_{CraFBP}\right) {x_{FBP}}^{p_{Cra,n}}}{{x_{FBP}}^{p_{Cra,n}} + {p_{Cra,K_{FBP}}}^{p_{Cra,n}}} - x_{CraFBP}\right]$$

$$f_{TF,Crp} = p_{Crp,scale}\left[\frac{\left(x_{Crp} + x_{CrpcAMP}\right) {x_{cAMP}}^{p_{Crp,n}}}{{x_{cAMP}}^{p_{Crp,n}} + {p_{Crp,K_{cAMP}}}^{p_{Crp,n}}} - x_{CrpcAMP}\right]$$

$$f_{TF,PdhR} = p_{PdhR,scale}\left[\frac{\left(x_{PdhR} + x_{PdhRPYR}\right) {x_{PYR}}^{p_{PdhR,n}}}{{x_{PYR}}^{p_{PdhR,n}} + {p_{PdhR,K_{PYR}}}^{p_{PdhR,n}}} - x_{PdhRPYR}\right] \quad .$$

The binding of Cra to FBP is assumed to be cooperative with degree $n = 2$, because Cra is structurally similar to LacI (both proteins belong to the GalR/LacI family of transcriptional regulators), which binds to lactose with $n \approx 2$ (Yagil & Yagil, 1971). The bindings of the other two interactions are assumed to be non-cooperative ($n = 1$), reducing their Hill-type kinetics to Michaelis-Menten-type.

The binding of the transcription factor IclR to the metabolites GLX and PYR is modeled jointly with the binding of IclR to the promoter region of the *aceBAK* operon, and is presented in Section 1.7.1. This modeling avoids the introduction of three additional states (IclR bound to either GLX or PYR or both) and the rates between these, and is straightforward because IclR represses only that one operon.

1.7 Gene expression

This section first describes the modeling of regulated gene expression, and then of unregulated gene expression. It continues with explaining how the growth rate dependency of gene expression was modeled, and, finally, lists the resulting rate equations.

1.7.1 Expression of regulated genes

The production rates of most modeled proteins are regulated by at least one of the four modeled transcription factors (known transcriptional regulations exerted by other transcription factors have been ignored, because these are outside the chosen system boundary, see Section 1.1 of this Supporting Information).

With two exceptions, the expression of a gene is regulated by only one transcription factor. In this case, the impact of transcriptional regulation on the protein production rate is modeled as a weighed sum of two production rates. These two production rates are quantified by the parameters $p_{<gene>,v_{<TF>,unbound}}$ and $p_{<gene>,v_{<TF>,bound}}$, respectively. The parameter $p_{<gene>,v_{<TF>,unbound}}$ quantifies the production rate when the promoter is not occupied by the regulating transcription factor; the parameter $p_{<gene>,v_{<TF>,bound}}$ quantifies the production rate when the promoter is occupied by the regulating transcription factor ('bound'). These two production rates are weighed by the occupancy of the promoter with the regulating transcription factor. To calculate the occupancy and thus the weighting factor, either a Michaelis-Menten or a Hill kinetics was used, with the regulating transcription factor's active form, i.e. Cra, Crp-cAMP, or PdhR (as opposed to their inactive forms Cra-FBP, Crp, and PdhR-PYR), as substrate. A Michaelis-Menten kinetics was preferred unless it was unable to reproduce the steady state rates on glucose and acetate; in these cases, we chose a Hill kinetics instead.

One of the two promoters regulated by more than one TF is that of the super-enzyme 'Emp'. The production of this enzyme, which represents the section of the Emden-Meyerhoff pathway between FBP and PG3, is transcriptionally activated by Crp and

repressed by Cra. The contributions of these two transcriptions factors to the overall expression rate are modeled as additive (as opposed to multiplicative).

The second promoter regulated by more than one TF is that of the *aceBAK* operon, which controls the production of the three enzymes AceA, AceB and AceK. The ratio of these three enzymes' production rates $f_{G,aceA} : f_{G,aceB} : f_{G,aceK}$ is approximately equal to $1 : 0.3 : 0.03$ (Chung et al, 1993). In the model, this ratio is ensured by first calculating the gene expression rate of *aceA*, and then scaling that rate with 0.3 and 0.03 to obtain the expression rates of the *aceB* and *aceK* genes, respectively. The expression of the *aceA* gene is jointly regulated by the three transcription factors Cra, Crp and IclR. The impact of these three individual regulations on the overall expression of the *aceA* gene is modeled as additive (as opposed to multiplicative).

The third of the three additive contributions to the overall expression rate of the *aceA* gene is its repression by the transcription factor IclR. The two ligands recognized by IclR act as corepressor (PYR) or activator (GLX) on the transcription of the *aceBAK* operon (Lorca et al, 2007), in the manner depicted in Figure S1. Thus, if one monitors the binding of DNA to the tetramer (T) in the absence and presence of pyruvate (P), which is opposed by glyoxylate (G), which binds to the dimer (D), the observed response Y is

$$Y = \frac{X\left[\frac{[DNA]}{K_{DNA}}\left(1+\frac{[P]}{K_P}\right)\right]}{(1+\frac{1}{L}\left[\frac{[G]}{K_G}\left(1+\frac{[G]}{K_G}\right)\right]+\frac{[DNA]}{K_{DNA}}+\frac{[P]}{K_P}+\frac{[DNA][P]}{K_{DNA}K'_P}} \quad ,$$

with X the maximum response and the equilibria defined in the caption of Figure S1.

Unlike the interaction of the other transcription factors with their respective ligands (see Section 1.6), the mechanistic description of IclR activity is directly incorporated into the expression rate equation of the *aceA* gene.

1.7.2 Expression of unregulated genes

Constitutively expressed enzymes, PTS proteins and transcription factors are, with two exceptions, modeled with a constant concentration. The production (see the Equations below), dilution and degradation rates (see Section 1.8) of these proteins are set to zero; therefore, the constant protein concentrations are determined by the initial conditions.

The two exceptions are the enzymes Ppc and MaeAB (which lumps the two isoenzymes MaeA and MaeB). Neither of the genes *ppc*, *maeA* nor *maeB* is known to be regulated (Keseler et al, 2009), yet, the respective mRNA concentrations were found to be markedly distinct for growth on glucose and acetate (Oh et al, 2002). As it has been observed that protein and mRNA abundances in *E. coli* cells are significantly correlated (Ishihama et al, 2008), the respective protein concentrations are very likely also markedly distinct. Accordingly, the measured steady state fluxes on glucose and acetate could not be simultaneously reproduced with constant Ppc and MaeAB concentrations.

Therefore, we set up the model equations in such a way that the differences in the Ppc and MaeAB concentrations on glucose and acetate are proportional to the measured differences in the respective mRNA concentrations. To realize such concentration changes

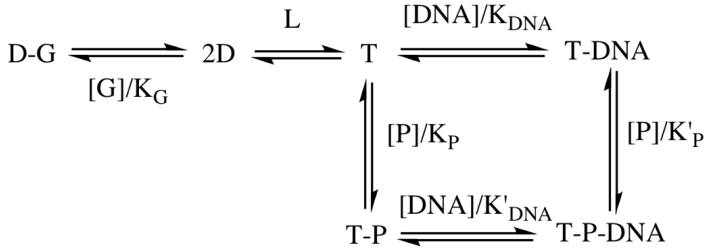

Figure S1: Graphical representation of the interactions described by (Lorca et al, 2007), from which the kinetic equation describing these interactions is derived. IcIR, as dimer (D) or tetramer (T), is being titrated by DNA, glyoxylate (G), and/or pyruvate (P). The equilibria needed for the derivation are $K_{DNA} = \frac{[T][DNA]}{[T-DNA]}$, $K_P = \frac{[T][P]}{[T-P]}$, $K'_P = \frac{[T-DNA][P]}{[T-P-DNA]}$, $K_G = \frac{[G][D]}{[G-D]}$ and $L = \frac{[T]}{[D]^2}$. As only three out of the four equilibria around a cycle are needed to define it, the remaining equilibrium $K'_{DNA} = \frac{[T-P][DNA]}{[T-P-DNA]}$ is not needed for the derivation of the kinetic equation.

as a response to changes in the availability of glucose and acetate, we chose the following implementation. First, for each of the two enzymes Ppc and MaeAB, the model calculates the sum of dilution and degradation rates that would occur if the Ppc and MaeAB concentrations were in steady state (for the calculation of the carbon source-dependent steady state concentrations SS_{Ppc} and SS_{MaeAB} of Ppc and MaeAB, respectively, see Section 1.9 of this Supporting Information). Then, the actual production rates of Ppc and MaeAB are set to equal their steady state degradation+dilution rates. The effect of this modeling is that the actual, possibly out-of-steady state protein concentrations x_{MaeAB} and x_{Ppc} approach their calculated, carbon source-dependent steady state concentrations. With this workaround, the model is capable to reproduce the measured steady state fluxes for growth on glucose and acetate.

1.7.3 Growth rate–dependency of gene expression

Gene expression is growth rate–dependent due to growth-rate dependent concentrations of DNA polymerases and ribosomes (Bremer et al, 2008). The growth-rate dependent efficiency of the gene expression machinery is modeled as a linear function of the growth rate ($p_{BM,k_{expr}} \cdot \mu$), and the expression rates of all regulated genes are multiplied by this function.

We found that when this growth rate-dependency is neglected, the measured steady state concentrations of the proteins cannot be reproduced on both glucose and acetate simultaneously. The reason for such failed reproduction is that to reproduce the measured steady states where the protein production and dilution+degradation rates are equal, the production rates must be capable to balance the dilution rates for both high and low growth rates. However, the model covers a wide range of growth rates (the growth rate on glucose is approximately three times higher than the growth rate on acetate); therefore, the inherently growth-rate dependent dilution rates can vary over

a wide range. To make the production rates capable to balance the dilution rates for both high and low growth rates, the growth-rate dependency of gene expression must be considered as well.

1.7.4 Rate equations for gene expression

Table S2 lists the chosen types of rate equations to describe the process of gene expression. The full equations follow this table.

Table S2: Overview of the chosen types of rate equations to describe the process of gene expression. The following abbreviations are used: MM – Michaelis-Menten kinetics plus basal expression term, Hill – Hill kinetics plus basal expression term, (A) – transcriptional activator, (R) – transcriptional repressor.

Rate	Type	Regulators
$f_{G,aceA}$	special, see text	Cra (A), Crp-cAMP (R), IclR (R)
$f_{G,aceB}$	$= 0.3 \cdot f_{G,aceA}$	—
$f_{G,aceK}$	$= 0.03 \cdot f_{G,aceA}$	—
$f_{G,acoa2act}$	$= 0$	—
$f_{G,acs}$	Hill	Crp-cAMP (A)
$f_{G,akg2mal}$	Hill	Crp-cAMP (A)
$f_{G,campdegr}$	$= 0$	—
$f_{G,cra}$	$= 0$	—
$f_{G,crp}$	$= 0$	—
$f_{G,cya}$	$= 0$	—
$f_{G,emp}$	MM	Cra (R), Crp-cAMP (A)
$f_{G,eno}$	MM	Cra (R)
$f_{G,fdp}$	MM	Cra (A)
$f_{G,gltA}$	Hill	Crp-cAMP (A)
$f_{G,icd}$	MM	Cra (A)
$f_{G,iclr}$	$= 0$	—
$f_{G,maeAB}$	special, see text	—
$f_{G,mdh}$	MM	Crp-cAMP (A)
$f_{G,pckA}$	MM	Cra (A)
$f_{G,pdh}$	MM	PdhR (R)
$f_{G,pdhr}$	$= 0$	—
$f_{G,pfkA}$	MM	Cra (R)
$f_{G,ppc}$	special, see text	—
$f_{G,ppsA}$	MM	Cra (A)
$f_{G,pykF}$	MM	Cra (R)
$f_{G,EIIA}$	$= 0$	—
$f_{G,EIICB}$	$= 0$	—

$$
\begin{aligned}
f_{G,aceA} = \mu\, p_{BM,k_{expr}} \Bigg\{ & \left(1 - \frac{x_{Cra}}{x_{Cra} + p_{aceBAK,K_{Cra}}}\right) p_{aceBAK,v_{Cra,unbound}} \cdots \\
& + \frac{x_{Cra}}{x_{Cra} + p_{aceBAK,K_{Cra}}}\, p_{aceBAK,v_{Cra,bound}} \cdots \\
& + \left(1 - \frac{x_{CrpcAMP}}{x_{CrpcAMP} + p_{aceBAK,K_{Crp}}}\right) p_{aceBAK,v_{Crp,unbound}} \cdots \\
& + \frac{x_{CrpcAMP}}{x_{CrpcAMP} + p_{aceBAK,K_{Crp}}}\, p_{aceBAK,v_{Crp,bound}} \cdots \\
& + \Bigg[1 - \frac{p_{aceBAK,DNA}}{p_{aceBAK,K_{DNA}}} \left(1 + \frac{x_{PYR}}{p_{aceBAK,K_{PYRprime}}}\right) \cdots \\
& \left(1 + \frac{1}{L} \left(\frac{x_{GLX}}{p_{aceBAK,K_{GLX}}}\right) \left(1 + \frac{x_{GLX}}{p_{aceBAK,K_{GLX}}}\right) \cdots \right. \\
& + \frac{p_{aceBAK,DNA}}{p_{aceBAK,K_{DNA}}} + \frac{x_{PYR}}{p_{aceBAK,K_{PYR}}} + \frac{p_{aceBAK,DNA}}{p_{aceBAK,K_{DNA}}} \cdots \\
& \left. \cdot \frac{x_{PYR}}{p_{aceBAK,K_{PYRprime}}}\right)^{-1} \Bigg]\, p_{aceBAK,k_{cat,IclR}}\, x_{IclR} \Bigg\} \\
f_{G,aceB} = {} & p_{aceBAK,aceBfactor}\, f_{G,aceA} \\
f_{G,aceK} = {} & p_{aceBAK,aceKfactor}\, f_{G,aceA} \\
f_{G,acoa2act} = {} & 0 \\
f_{G,acs} = {} & \mu\, p_{BM,k_{expr}} \Bigg[\left(1 - \frac{x_{CrpcAMP}{}^{p_{acs,n}}}{x_{CrpcAMP}{}^{p_{acs,n}} + p_{acs,K_{Crp}}{}^{p_{acs,n}}}\right) p_{acs,v_{Crp,unbound}} \cdots \\
& + \frac{x_{CrpcAMP}{}^{p_{acs,n}}}{x_{CrpcAMP}{}^{p_{acs,n}} + p_{acs,K_{Crp}}{}^{p_{acs,n}}}\, p_{acs,v_{Crp,bound}} \Bigg] \\
f_{G,akg2mal} = {} & \mu\, p_{BM,k_{expr}} \Bigg[\left(1 - \frac{x_{CrpcAMP}{}^{p_{akg2mal,n}}}{x_{CrpcAMP}{}^{p_{akg2mal,n}} + p_{akg2mal,K_{Crp}}{}^{p_{akg2mal,n}}}\right) \cdots \\
& p_{akg2mal,v_{Crp,unbound}} + \frac{x_{CrpcAMP}{}^{p_{akg2mal,n}}}{x_{CrpcAMP}{}^{p_{akg2mal,n}} + p_{akg2mal,K_{Crp}}{}^{p_{akg2mal,n}}} \cdots \\
& p_{akg2mal,v_{Crp,bound}} \Bigg] \\
f_{G,campdegr} = {} & 0 \\
f_{G,cra} = {} & 0 \\
f_{G,crp} = {} & 0 \\
f_{G,cya} = {} & 0
\end{aligned}
$$

$$
\begin{aligned}
f_{G,emp} &= \mu\, p_{BM,k_{expr}} \left[\left(1 - \frac{x_{Cra}}{x_{Cra} + p_{emp,K_{Cra}}} \right) p_{emp,v_{Cra,unbound}} \cdots \right. \\
&\quad + \frac{x_{Cra}}{x_{Cra} + p_{emp,K_{Cra}}}\, p_{emp,v_{Cra,bound}} \cdots \\
&\quad + \left(1 - \frac{x_{CrpcAMP}}{x_{CrpcAMP} + p_{emp,K_{Crp}}} \right) p_{emp,v_{Crp,unbound}} \cdots \\
&\quad \left. + \frac{x_{CrpcAMP}}{x_{CrpcAMP} + p_{emp,K_{Crp}}}\, p_{emp,v_{Crp,bound}} \right] \\
f_{G,eno} &= \mu\, p_{BM,k_{expr}} \left[\left(1 - \frac{x_{Cra}}{x_{Cra} + p_{eno,K_{Cra}}} \right) p_{eno,v_{Cra,unbound}} \cdots \right. \\
&\quad \left. + \frac{x_{Cra}}{x_{Cra} + p_{eno,K_{Cra}}}\, p_{eno,v_{Cra,bound}} \right] \\
f_{G,fdp} &= \mu\, p_{BM,k_{expr}} \left[\left(1 - \frac{x_{Cra}}{x_{Cra} + p_{fdp,K_{Cra}}} \right) p_{fdp,v_{Cra,unbound}} \cdots \right. \\
&\quad \left. + \frac{x_{Cra}}{x_{Cra} + p_{fdp,K_{Cra}}}\, p_{fdp,v_{Cra,bound}} \right] \\
f_{G,gltA} &= \mu\, p_{BM,k_{expr}} \left[\left(1 - \frac{x_{CrpcAMP}{}^{p_{gltA,n}}}{x_{CrpcAMP}{}^{p_{gltA,n}} + p_{gltA,K_{Crp}}{}^{p_{gltA,n}}} \right) p_{gltA,v_{Crp,unbound}} \cdots \right. \\
&\quad \left. + \frac{x_{CrpcAMP}{}^{p_{gltA,n}}}{x_{CrpcAMP}{}^{p_{gltA,n}} + p_{gltA,K_{Crp}}{}^{p_{gltA,n}}}\, p_{gltA,v_{Crp,bound}} \right] \\
f_{G,icd} &= \mu\, p_{BM,k_{expr}} \left[\left(1 - \frac{x_{Cra}}{x_{Cra} + p_{icd,K_{Cra}}} \right) p_{icd,v_{Cra,unbound}} \cdots \right. \\
&\quad \left. + \frac{x_{Cra}}{x_{Cra} + p_{icd,K_{Cra}}}\, p_{icd,v_{Cra,bound}} \right] \\
f_{G,iclr} &= 0 \\
f_{G,maeAB} &= (\mu + p_{D,k_{degr}})\, SS_{x_{MaeAB}} \\
f_{G,mdh} &= \mu\, p_{BM,k_{expr}} \left[\left(1 - \frac{x_{CrpcAMP}}{x_{CrpcAMP} + p_{mdh,K_{Crp}}} \right) p_{mdh,v_{Crp,unbound}} \cdots \right. \\
&\quad \left. + \frac{x_{CrpcAMP}}{x_{CrpcAMP} + p_{mdh,K_{Crp}}}\, p_{mdh,v_{Crp,bound}} \right] \\
f_{G,pckA} &= \mu\, p_{BM,k_{expr}} \left[\left(1 - \frac{x_{Cra}}{x_{Cra} + p_{pckA,K_{Cra}}} \right) p_{pckA,v_{Cra,unbound}} \cdots \right.
\end{aligned}
$$

$$
\begin{aligned}
&\quad + \frac{x_{Cra}}{x_{Cra} + p_{pckA,K_{Cra}}} p_{pckA,v_{Cra,bound}} \Bigg] \\
f_{G,pdh} &= \mu\, p_{BM,k_{expr}} \left[\left(1 - \frac{x_{PdhR}}{x_{PdhR} + p_{pdh,K_{PdhR}}} \right) p_{pdh,v_{PdhR,unbound}} \cdots \right. \\
&\quad \left. + \frac{x_{PdhR}}{x_{PdhR} + p_{pdh,K_{PdhR}}} p_{pdh,v_{PdhR,bound}} \right] \\
f_{G,pdhr} &= 0 \\
f_{G,pfkA} &= \mu\, p_{BM,k_{expr}} \left[\left(1 - \frac{x_{Cra}}{x_{Cra} + p_{pfkA,K_{Cra}}} \right) p_{pfkA,v_{Cra,unbound}} \cdots \right. \\
&\quad \left. + \frac{x_{Cra}}{x_{Cra} + p_{pfkA,K_{Cra}}} p_{pfkA,v_{Cra,bound}} \right] \\
f_{G,ppc} &= (\mu + p_{D,k_{degr}})\, SS_{x_{Ppc}} \\
f_{G,ppsA} &= \mu\, p_{BM,k_{expr}} \left[\left(1 - \frac{x_{Cra}}{x_{Cra} + p_{ppsA,K_{Cra}}} \right) p_{ppsA,v_{Cra,unbound}} \cdots \right. \\
&\quad \left. + \frac{x_{Cra}}{x_{Cra} + p_{ppsA,K_{Cra}}} p_{ppsA,v_{Cra,bound}} \right] \\
f_{G,pykF} &= \mu\, p_{BM,k_{expr}} \left[\left(1 - \frac{x_{Cra}}{x_{Cra} + p_{pykF,K_{Cra}}} \right) p_{pykF,v_{Cra,unbound}} \cdots \right. \\
&\quad \left. + \frac{x_{Cra}}{x_{Cra} + p_{pykF,K_{Cra}}} p_{pykF,v_{Cra,bound}} \right] \\
f_{G,EIIA} &= 0 \\
f_{G,EIICB} &= 0
\end{aligned}
$$

1.8 Dilution and degradation of compounds

All metabolites dilute with the growth rate due to the expanding volume of the cell. Similarly, proteins dilute in the same manner, and additionally degrade with a here assumed 'universal' protein degradation rate k_{degr}. The concentrations of some proteins such as the transcription factors, however, are assumed as constant; these proteins are in the model neither produced (see Section 1.7.2), nor diluted or degraded.

Metabolite dilution

$$f_{D,ACoA} = \mu\, x_{ACoA}$$
$$f_{D,cAMP} = \mu\, x_{cAMP}$$
$$f_{D,FBP} = \mu\, x_{FBP}$$
$$f_{D,G6P} = \mu\, x_{G6P}$$
$$f_{D,GLX} = \mu\, x_{GLX}$$
$$f_{D,ICT} = \mu\, x_{ICT}$$
$$f_{D,MAL} = \mu\, x_{MAL}$$
$$f_{D,OAA} = \mu\, x_{OAA}$$
$$f_{D,PEP} = \mu\, x_{PEP}$$
$$f_{D,PG3} = \mu\, x_{PG3}$$
$$f_{D,PYR} = \mu\, x_{PYR}$$
$$f_{D,AKG} = \mu\, x_{AKG}$$

Protein degradation and dilution

$$f_{D,AceA} = (\mu + p_{D,k_{degr}})\, x_{AceA}$$
$$f_{D,AceB} = (\mu + p_{D,k_{degr}})\, x_{AceB}$$
$$f_{D,AceK} = (\mu + p_{D,k_{degr}})\, x_{AceK}$$
$$f_{D,Acoa2act} = 0$$
$$f_{D,Acs} = (\mu + p_{D,k_{degr}})\, x_{Acs}$$
$$f_{D,CAMPdegr} = 0$$
$$f_{D,Cra} = 0$$
$$f_{D,CraFBP} = 0$$
$$f_{D,Crp} = 0$$
$$f_{D,CrpcAMP} = 0$$
$$f_{D,Cya} = 0$$
$$f_{D,Emp} = (\mu + p_{D,k_{degr}})\, x_{Emp}$$
$$f_{D,Eno} = (\mu + p_{D,k_{degr}})\, x_{Eno}$$
$$f_{D,Fdp} = (\mu + p_{D,k_{degr}})\, x_{Fdp}$$
$$f_{D,GltA} = (\mu + p_{D,k_{degr}})\, x_{GltA}$$
$$f_{D,Icd} = (\mu + p_{D,k_{degr}})\, x_{Icd}$$
$$f_{D,Icd-P} = (\mu + p_{D,k_{degr}})\, x_{Icd-P}$$
$$f_{D,IclR} = 0$$
$$f_{D,MaeAB} = (\mu + p_{D,k_{degr}})\, x_{MaeAB}$$
$$f_{D,Mdh} = (\mu + p_{D,k_{degr}})\, x_{Mdh}$$

$$
\begin{aligned}
f_{D,PckA} &= (\mu + p_{D,k_{degr}})\, x_{PckA} \\
f_{D,Pdh} &= (\mu + p_{D,k_{degr}})\, x_{Pdh} \\
f_{D,PdhR} &= 0 \\
f_{D,PdhRPYR} &= 0 \\
f_{D,PfkA} &= (\mu + p_{D,k_{degr}})\, x_{PfkA} \\
f_{D,Ppc} &= (\mu + p_{D,k_{degr}})\, x_{Ppc} \\
f_{D,PpsA} &= (\mu + p_{D,k_{degr}})\, x_{PpsA} \\
f_{D,PykF} &= (\mu + p_{D,k_{degr}})\, x_{PykF} \\
f_{D,Akg2mal} &= (\mu + p_{D,k_{degr}})\, x_{Akg2mal} \\
f_{D,EIIA} &= 0 \\
f_{D,EIIA_P} &= 0 \\
f_{D,EIICB} &= 0
\end{aligned}
$$

1.9 Biomass production rates and growth rate calculation

Calculation of growth rates from simulated intracellular concentrations and reaction rates (such as of the biomass–producing metabolic reactions) is still an unresolved problem in the field of kinetic models. A previous study was unable to find a function that reproduces the measured growth rates from the simulated compound concentrations and reaction rates (Bettenbrock et al, 2006). Instead, the authors of this work used the measured time course of the growth rate as input to the model. The same group has later established a correlation between the growth rate on glycolytic substrates and the phosphorylation of a PTS protein (Bettenbrock et al, 2007), which the here presented model unfortunately cannot exploit since this correlation only holds for glycolytic growth but not for growth on the gluconeogenic substrate acetate.

In this study, we chose a different approach to calculate the growth rate. Instead of calculating the growth rate as a function of the intracellular states and rates, we exploited the fact that the growth rate is determined by the quality of the growth medium (Tao et al, 1999) and calculated the growth rate as a function of the available carbon sources. This function uses two weights that depend on the available carbon sources to interpolate between the steady state growth rates on either glucose or acetate as the sole carbon sources.

The two weights used to calculate the carbon source-dependent growth rate are defined as

$$
\begin{aligned}
\alpha_{GLC} &= \frac{x_{GLC}}{x_{GLC} + p_{PTS,K_{GLC}}} \\
\alpha_{ACT} &= \frac{x_{ACT}}{x_{ACT} + p_{Acs,K_{ACT}}} \left(1 - \alpha_{GLC}\right) ,
\end{aligned}
$$

with $p_{PTS,K_{GLC}}$ the Monod constant for glucose and $p_{Acs,K_{ACT}}$ the Monod constant for acetate. With this definition, α_{GLC} vanishes when glucose is absent and approaches 1 for

increasing glucose concentrations, α_{ACT} vanishes when acetate is absent and approaches 1 for increasing acetate concentrations only when glucose is absent, and $0 \leq \alpha_{GLC} + \alpha_{ACT} < 1$. These two weigths are then used to calculate the growth rate from the available carbon sources through

$$\mu = \alpha_{GLC}\, p_{BM,\mu_{GLC}} + \alpha_{ACT}\, p_{BM,\mu_{ACT}} \ , \tag{S1}$$

which interpolates between the known growth rates on glucose ($p_{BM,\mu_{GLC}}$) and acetate ($p_{BM,\mu_{ACT}}$).

The two weights α_{GLC} and α_{ACT} are further used to calculate the carbon source-dependent steady state concentrations $SS_{x_{Ppc}}$ and $SS_{x_{MaeAB}}$ of the enzymes Ppc and MaeAB (see Section 1.7.2) through

$$\begin{aligned} SS_{x_{MaeAB}} &= \alpha_{GLC} \cdot 1.00 \cdot 10^{-3} \frac{g_{Prot}}{g_{DW}} + \alpha_{ACT} \cdot 3.40 \cdot 10^{-3} \frac{g_{Prot}}{g_{DW}} \\ SS_{x_{Ppc}} &= \alpha_{GLC} \cdot 1.00 \cdot 10^{-3} \frac{g_{Prot}}{g_{DW}} + \alpha_{ACT} \cdot 2.80 \cdot 10^{-4} \frac{g_{Prot}}{g_{DW}} \ , \end{aligned}$$

which interpolate between the steady state data on glucose and acetate.

The reactions for the production of biomass from the seven precursor metabolites ACoA, AKG, G6P, OAA, PEP, PG3 and PYR are modeled with first order kinetics,

$$\begin{aligned} f_{BM,ACoA} &= k_{BM,ACoA}\, x_{ACoA} \\ f_{BM,AKG} &= k_{BM,AKG}\, x_{AKG} \\ f_{BM,G6P} &= k_{BM,G6P}\, x_{G6P} \\ f_{BM,OAA} &= k_{BM,OAA}\, x_{OAA} \\ f_{BM,PEP} &= k_{BM,PEP}\, x_{PEP} \\ f_{BM,PG3} &= k_{BM,PG3}\, x_{PG3} \\ f_{BM,PYR} &= k_{BM,PYR}\, x_{PYR} \ , \end{aligned}$$

with $k_{BM,M}$ the seven first order reaction rate constants. These rate constants were determined as follows. At steady state, the seven biomass production rates $f_{BM,M,SS}$ and the seven metabolite concentrations $x_{M,SS}$ are known for growth on either glucose or acetate (see Section 2). Thus, the carbon source-dependent first order rate constants are given by $k_{BM,M} = f_{BM,M,SS}/x_{M,SS}$. As these rate constants differ for growth on glucose or acetate, their actual values depend on the available carbon sources and are determined through

$$\begin{aligned} k_{BM,ACoA} &= \alpha_{GLC}\, p_{BM,GLC_{ACoA}} + \alpha_{ACT}\, p_{BM,ACT_{ACoA}} \\ k_{BM,AKG} &= \alpha_{GLC}\, p_{BM,GLC_{AKG}} + \alpha_{ACT}\, p_{BM,ACT_{AKG}} \\ k_{BM,G6P} &= \alpha_{GLC}\, p_{BM,GLC_{G6P}} + \alpha_{ACT}\, p_{BM,ACT_{G6P}} \\ k_{BM,OAA} &= \alpha_{GLC}\, p_{BM,GLC_{OAA}} + \alpha_{ACT}\, p_{BM,ACT_{OAA}} \\ k_{BM,PEP} &= \alpha_{GLC}\, p_{BM,GLC_{PEP}} + \alpha_{ACT}\, p_{BM,ACT_{PEP}} \\ k_{BM,PG3} &= \alpha_{GLC}\, p_{BM,GLC_{PG3}} + \alpha_{ACT}\, p_{BM,ACT_{PG3}} \\ k_{BM,PYR} &= \alpha_{GLC}\, p_{BM,GLC_{PYR}} + \alpha_{ACT}\, p_{BM,ACT_{PYR}} \ , \end{aligned}$$

which interpolate between the carbon source-dependent first order rate constants on glucose p_{BM,GLC_M} and acetate p_{BM,ACT_M}.

2 Parameter estimation

This section first outlines the followed parameter estimation strategy. Then, it describes the derivation of complete state and rate data sets, which need to be determined in order to apply the chosen parameter estimation strategy. Finally, it lists the values of the estimated parameters.

2.1 Application of the divide–and–conquer approach

We applied the divide–and–conquer approach (Kotte & Heinemann, 2009) to determine the parameters of the presented model from experimental data. This approach decomposes the global estimation problem into multiple independent subproblems of much smaller dimension. This property effectively removes the burden of providing a global optimizer with sufficiently good initial guesses of the parameter values, which is a significant relief given the size of this estimation problem.

In the first step of the divide–and–conquer approach, complete steady state -omics data sets of all the model's states and rates must be obtained. However, the available -omics measurement data sets are still incomplete. Therefore, we needed to incorporate additional biological knowledge in order to 'extrapolate' these incomplete measurement data sets to complete data sets of observables. Based on published measurement data, we derived two complete data sets for balanced growth on glucose and acetate, respectively. For details on this derivation, refer to Sections 2.2 and 2.3. The two complete data sets comprise 153 data points each, or 306 in total — 2 x 44 data points of states (see Table S3), and 2 x 109 data points of rates (see Table S4).

The second step in the application of the divide–and–conquer approach is the decomposition of the global estimation problem into multiple independent subproblems of smaller dimension. The degree of this decomposition, and thus the advantage of using the approach, can be increased by ensuring that each *estimated* parameter appears in exactly one rate equation. In the model, all parameters appear in exactly one rate equation, with the exception of two: The universal protein degradation rate $p_{D,k_{degr}}$ appears in all dynamic protein degradation rate equations, and the scaling factor of the growth-rate dependent efficiency of the gene expression machinery $p_{BM,k_{expr}}$ appears in all dynamic gene expression rate equations. If these two parameters are excluded from the estimation problem, then the estimation problems of all rates become independent of each other. In order to trigger such a decomposition, we excluded these two parameter from the estimation problem. Instead, we used a literature value for the universal protein degradation rate $p_{D,k_{degr}}$ and arbitrarily set the scaling factor of the growth-rate dependent efficiency of the gene expression machinery $p_{D,k_{degr}}$ to 1. This arbitrary value is justified because in the model, $p_{D,k_{degr}}$ is always multiplied with parameters that describe the maximal gene expression rates, such that the later estimation of these maximal gene expression rates can correct for the arbitrary value of $p_{D,k_{degr}}$. With the exclusion of these two parameters from the estimation problem, the estimation problems of the individual rate equations are decoupled from each other and can thus be solved independently.

The third and final fourth steps of the divide–and–conquer approach concern the derivation of the complete, analytical solution spaces of the exactly determined or underdetermined parameter estimation subproblems, and the systematic analysis of these spaces to obtain a sound system understanding in the face of non-identifiable parameter values (Kotte & Heinemann, 2009). When an estimation subproblem was underdetermined, we screened the literature and two previous models (Bettenbrock et al, 2006; Chassagnole et al, 2002) for values of parameters that appear in the underdetermined subproblem. The solutions to the small dimensional estimation subproblems were then joined to the solution of the original parent estimation problem. The resulting parameter values are listed in Table S5.

2.2 Derivation of complete data sets of state variables

Table S3 contains the steady state values of the state variables $\mathbf{x}$ on glucose and acetate. These values are either experimental data, or, where experimental data was not available, estimated from experimental data through the inclusion of additional biological knowledge. Specifically, to obtain two complete metabolomes, we used NET analysis (Kümmel et al, 2006) to integrate and consolidate quantitative metabolite measurements from multiple sources (Lowry et al, 1971; Chassagnole et al, 2002; Epstein et al, 1975; el-Mansi et al, 1986; Crasnier-Mednansky, 1997; Peng et al, 2004; Rahman et al, 2006), measured during growth on either glucose or acetate, into two thermodynamically consistent data sets. To complete these data sets, we again used NET analysis to infer unknown metabolite concentrations from measured concentrations.

To obtain a complete proteome for balanced growth on glucose, we used measured concentrations where available (Ishihama et al, 2008; Anderson et al, 1971) and set all unmeasured protein concentrations to the arbitrary value $1.0 \cdot 10^{-3} g_{Prot}/g_{DW}$. These arbitrary protein concentrations on glucose are justified because in the model, a protein concentration always appears paired with a multiplicative parameter k_{cat} such that the later estimation of this parameter value can correct for an arbitrarily chosen absolute concentration of the protein. Unfortunately, we could not find any published proteome data for growth on acetate. However, it has been observed that protein and mRNA abundances in *E. coli* cells are significantly correlated (Ishihama et al, 2008). Therefore, we used the data of a microarray study that determined the ratios of mRNA concentrations between growth on glucose and acetate (Oh & Liao, 2000; Oh et al, 2002) to estimate the protein concentrations on acetate from those on glucose.

In five cases (EIIA, Icd, Cra, Crp, and PdhR), the concentration of a physical compound is distributed over two state variables. In these cases, the total concentration of the physical compound is the sum of these two state variables. Two of these cases arise because the PTS protein EIIA and the enzyme Icd both exist in a phosphorylated and an unphosphorylated form. As the degree of phosphorylation ρ with $0 \leq \rho \leq 1$ of these compounds is known for balanced growth on glucose and acetate (Bettenbrock et al, 2006; Walsh & Koshland, 1984), the steady state concentrations of the phosphorylated and unphosphorylated forms, x_p and x_u respectively, can be calculated from the total protein concentrations x_{tot} through $x_p = \rho\, x_{tot}$ and $x_u = (1 - \rho)\, x_{tot}$. The remaining

three cases arise because the TFs Cra, Crp, and PdhR appear either bound or unbound to their respective metabolite effectors FBP, cAMP, and PYR. Because the concentrations of the metabolite-bound and free forms on glucose and acetate are unknown, we needed a rationale to set these concentrations. As the activity of these TFs is believed to be markedly distinct during glycolytic and gluconeogenic growth, and the TF activities are modulated by their small molecule effectors, we chose the parameters quantifying the TF-metabolite bindings such that the difference between the TFs' metabolite-bound concentrations on glucose and acetate is maximized.

Table S3: Comprehensive list of the dynamic state variables $\mathbf{x}$, the full names of the represented compounds, and the steady state values on glucose and acetate, which are based on experimental data. The units of the states are $g\,l^{-1}$ for carbon sources, $\frac{\mu mol}{g_{DW}}$ for metabolites, $\frac{g_{Prot}}{g_{DW}}$ for proteins, and $[OD]$ for the biomass concentration.

Name of state	Description	Data on glucose	Data on acetate
x_{OD}	Biomass concentration	-	-
x_{ACT}	Extracellular acetate	-	-
x_{GLC}	Extracellular glucose	-	-
x_{ACoA}	Acetyl-CoA	0.35	1.9
x_{AKG}	α-Ketoglutarate	0.2	1.1
x_{cAMP}	Cyclic AMP	0.2	4
x_{FBP}	Fructose-1,6-bisphosphate	6.6	0.28
x_{G6P}	Glucose-6-phosphate	1.85	1.17
x_{GLX}	Glyoxylate	1.00E-08	1.35
x_{ICT}	Isocitrate	1.35E-03	1.54
x_{MAL}	Malate	3.6	6.65
x_{OAA}	Oxaloacetate	0.05	0.07
x_{PEP}	Phosphoenolpyruvate	0.21	0.59
x_{PG3}	3-Phosphoglycerate	5.75	1.35
x_{PYR}	Pyruvate	0.9	0.03
x_{AceA}	Isocitrate lyase	4.68E-03	1.03E-01
x_{AceB}	Malate synthase A	1.40E-03	3.09E-02
x_{AceK}	Isocitrate dehydrogenase phosphatase/kinase	1.40E-04	3.09E-03
$x_{Acoa2act}$	Enzyme for the reaction from ACoA to ACT	1.00E-03	3.00E-04
x_{Acs}	Acetyl-CoA synthetase	3.62E-05	3.35E-04
$x_{Akg2mal}$	Enzyme for the reaction from AKG to MAL	1.00E-03	2.10E-03
$x_{CAMPdegr}$	Degradation of cAMP	1.00E-03	1.00E-03

continued on the next page ...

... Table S3 continued.

Name of state	Description	Data on glucose	Data on acetate
x_{Cya}	Adenylate cyclase	1.00E-03	1.00E-03
x_{Emp}	Enzyme for the reversible reaction between FBP and PG3	1.14E-02	9.64E-03
x_{Eno}	Enolase	1.14E-02	6.21E-03
x_{Fdp}	Fructose-1,6-bisphosphatase I	7.48E-05	2.44E-04
x_{GltA}	Citrate synthase	2.93E-04	1.01E-03
x_{Icd}	Unphosphorylated isocitrate dehydrogenase	4.28E-03	2.47E-03
x_{Icd-P}	Phosphorylated isocitrate dehydrogenase	1.78E-04	7.41E-03
x_{MaeAB}	Malic enzymes MaeAB	1.00E-03	3.40E-03
x_{Mdh}	Malate dehydrogenase	4.91E-04	1.56E-03
x_{PckA}	Phosphoenolpyruvate carboxykinase	3.37E-04	2.78E-03
x_{Pdh}	Pyruvate dehydrogenase	1.00E-03	3.79E-04
x_{PfkA}	6-phosphofructokinase I	2.42E-04	1.50E-04
x_{Ppc}	Phosphoenolpyruvate carboxylase	3.78E-04	1.06E-04
x_{PpsA}	Phosphoenolpyruvate synthase	1.00E-03	1.30E-02
x_{PykF}	Pyruvate kinase I	2.50E-03	5.47E-04
x_{EIIA}	Unphosphorylated PTS protein EIIA	9.65E-02	1.99E-03
x_{EIIA-P}	Phosphorylated PTS protein EIIA	3.48E-03	9.80E-02
x_{EIICB}	PTS protein EIICB	3.00E-03	3.00E-03
x_{Cra}	Free Cra	2.97E-04	6.99E-03
x_{CraFBP}	Cra bound to fructose-1,6-bisphosphate	6.99E-03	2.97E-04
x_{Crp}	Free Crp	5.96E-03	1.33E-03
$x_{CrpcAMP}$	Crp bound to cyclic AMP	1.33E-03	5.96E-03
x_{IclR}	IclR	7.29E-03	7.29E-03
x_{PdhR}	free PdhR	1.13E-03	6.17E-03
$x_{PdhRPYR}$	PdhR bound to pyruvate	6.17E-03	1.13E-03

2.3 Derivation of complete data sets of rates

Table S4 lists the values of the steady state rates $\mathbf{f}$ on glucose and acetate. These values are either experimental data, or, where experimental data was not available, estimated from experimental data through the inclusion of additional biological knowledge.

Two complete sets of metabolic reaction rates (covering the rates $\mathbf{f_E}$, $\mathbf{f_{PTS}}$ and $\mathbf{f_{BM}}$) were provided by the results of ^{13}C tracer experiments on glucose (Fuhrer et al, 2005) and acetate (Zhao et al, 2004).

To obtain two complete data sets of dilution rates $\mathbf{f_{dil}}$ of the compounds $\mathbf{x}$ due to cell growth, we used the model $\mathbf{f_{dil}} = \mu\,\mathbf{x}$ to calculate the dilution rates from the steady state concentrations of the proteins and metabolites on glucose and acetate, and from the known growth rate μ on these substrates. Similarly, to obtain two complete data sets of degradation rates $\mathbf{f_{degr}}$ of the proteins $\mathbf{x}$, we used the model $\mathbf{f_{degr}} = p_{D,k_{degr}}\,\mathbf{x}$ to calculate the degradation rates from the steady state protein concentrations on glucose and acetate, assuming the same degradation rate $p_{D,k_{degr}}$ for all proteins. The protein dilution and degradation rates, together with the steady state assumption $\mathbf{f_G} = \mathbf{f_{dil}} + \mathbf{f_{degr}}$, are used to calculate the steady state gene expression rates $\mathbf{f_G}$ on glucose and acetate.

The concentrations of the proteins EIIA and Icd are distributed over two state variables; one of these variables denotes the phosphorylated form, and the other the unphosphorylated form. Because the degrees of phosphorylation of the proteins EIIA and Icd have been determined experimentally (Bettenbrock et al, 2006; Walsh & Koshland, 1984), the *ratio* of the these proteins' steady state phosphorylation and dephosphorylation rates *between growth on glucose and acetate* is also known. However, the *magnitudes* of these rates are uncertain. We observed in preliminary simulations that the phosphorylation and dephosphorylation rates need to be sufficiently fast to not introduce oscillations into the metabolic network. Therefore, we set the steady state phosphorylation and desphosphorylation rates of the proteins EIIA and Icd to sufficiently high magnitudes in order to avoid such oscillations.

Similarly, as the steady state concentrations of the effector-bound and free forms of the transcription factors Cra, Crp, and PdhR have been estimated in Section 2.2, the ratios of these two forms' concentrations between growth on glucose and acetate are also known. Therefore, the ratios of both the association and dissociation rates between growth on glucose and acetate are known; however, the magnitudes of these rates are uncertain. In order to allow the binding states of the transcription factors to track the metabolite concentrations, the ratio of association and dissociation rates was scaled to the metabolic time scale, which is significantly faster than the slow time scale on which the TF's regulation of gene expression operates.

Table S4: Comprehensive list of the steady state rates $\mathbf{f}$. The units of the rates are h^{-1} for the growth rates; $\frac{g}{l \cdot s}$ for the substrate uptake and excretion rates of the cell population; $\frac{\mu mol}{g_{DW} \cdot s}$ for the enzymatic reaction rates $f_{E,\cdot}$ (except the AceK kinase and phosphatase reactions), for the PTS reactions $f_{PTS,\cdot}$, for the dilution rates of metabolites $f_{D,\cdot}$, for the association and dissociation rates of transcription factors to metabolites $f_{TF,\cdot}$, and for the biomass production rates $f_{BM,\cdot}$; $\frac{g_{Prot}}{g_{DW} \cdot s}$ for the AceK kinase and phosphatase reactions, for the gene expression rates $f_{G,\cdot}$ and for the protein dilution+degradation rates $f_{D,\cdot}$.

Name of rate	Description	Data on glucose	Data on acetate
$f_{ENV,growth}$	Growth rate	0.64	0.20
$f_{ENV,GLCup}$	Glucose uptake rate of the population	-	-
$f_{ENV,ACTup}$	Acetate uptake rate of the population	-	-
$f_{ENV,ACTex}$	Acetate excretion rate of the population	-	-
$f_{E,AceA}$	Metabolic flux through AceA	3.52E-04	0.666
$f_{E,AceB}$	Metabolic flux through AceB	3.52E-04	0.666
$f_{E,AceK-Ki}$	Rate of the AceK-kinase reaction	6.61E-04	1.91E-02
$f_{E,AceK-Ph}$	Rate of the AceK-phosphatase reaction	6.61E-04	1.91E-02
$f_{E,Acoa2act}$	Metabolic flux through Acoa2act, Cell dry weight-normalized acetate excretion rate	1.33	0.25
$f_{E,Acs}$	Metabolic flux through Acs, Cell dry weight-normalized acetate uptake rate	0	3.45
$f_{E,Akg2mal}$	Conversion rate of AKG to MAL	0.443	2.32
$f_{E,CAMPdegr}$	Degradation rate of cAMP	0.667	0.976
$f_{E,Cya}$	Production rate of cAMP	0.667	0.976
$f_{E,Emp}$	Conversion rate between FBP and PG3	3.87	-0.188
$f_{E,Eno}$	Metabolic flux through Eno	3.59	-0.277
$f_{E,Fdp}$	Metabolic flux through Fdp	3.00E-02	9.89E-02
$f_{E,GltA}$	Metabolic flux through GltA	0.570	2.38
$f_{E,Icd}$	Metabolic flux through Icd	0.569	1.717
$f_{E,MaeAB}$	Metabolic flux through MaeAB	6.88E-02	0.227
$f_{E,Mdh}$	Metabolic flux through Mdh	0.443	2.76
$f_{E,PckA}$	Metabolic flux through PckA	2.58E-02	0.282

continued on the next page ...

... Table S4 continued.

Name of state	Description	Data on glucose	Data on acetate
$f_{E,Pdh}$	Metabolic flux through Pdh	2.484	5.50E-02
$f_{E,PfkA}$	Metabolic flux through PfkA	1.966	1.00E-02
$f_{E,Ppc}$	Metabolic flux through Ppc	0.610	3.20E-03
$f_{E,PpsA}$	Metabolic flux through PpsA	1.30E-03	1.61E-02
$f_{E,PykF}$	Metabolic flux through PykF	0.695	1.00E-04
f_{PTS,r_1}	Metabolic flux through the PTS reaction r_1	2.22	0
f_{PTS,r_4}	Metabolic flux through the PTS reaction r_4, Cell dry weight-normalized glucose uptake rate	2.22	0
$f_{TF,Cra}$	Combined association & dissociation rates between Cra and FBP	0	0
$f_{TF,Crp}$	Combined association & dissociation rates between Crp and cAMP	0	0
$f_{TF,PdhR}$	Combined association & dissociation rates between PdhR and PYR	0	0
$f_{G,aceA}$	aceA expression rate	9.63E-07	8.61E-06
$f_{G,aceB}$	aceB expression rate	2.89E-07	2.58E-06
$f_{G,aceK}$	aceK expression rate	2.89E-08	2.58E-07
$f_{G,acoa2act}$	acoa2act expression rate	0	0
$f_{G,acs}$	acs expression rate	7.53E-09	2.81E-08
$f_{G,akg2mal}$	akg2mal expression rate	2.06E-07	1.75E-07
$f_{G,campdegr}$	campdegr expression rate	0	0
$f_{G,cra}$	cra expression rate	0	0
$f_{G,crp}$	crp axpression rate	0	0
$f_{G,cya}$	cya expression rate	0	0
$f_{G,EIIA}$	eiia expression rate	0	0
$f_{G,EIICB}$	eiicb expression rate	0	0
$f_{G,emp}$	emp expression rate	2.37E-06	8.10E-07
$f_{G,eno}$	eno expression rate	2.37E-06	5.22E-07
$f_{G,fdp}$	fdp expression rate	1.56E-08	2.05E-08
$f_{G,gltA}$	gltA expression rate	6.09E-08	8.45E-08
$f_{G,icd}$	icd expression rate	9.17E-07	8.26E-07
$f_{G,maeAB}$	maeAB expression rate	2.06E-07	2.84E-07

continued on the next page ...

... Table S4 continued.

Name of state	Description	Data on glucose	Data on acetate
$f_{G,iclr}$	iclr expression rate	0	0
$f_{G,mdh}$	mdh expression rate	1.02E-07	1.31E-07
$f_{G,pckA}$	pckA expression rate	7.01E-08	2.34E-07
$f_{G,pdh}$	pdh expression rate	2.08E-07	3.18E-08
$f_{G,pdhr}$	pdhR expression rate	0	0
$f_{G,pfkA}$	pfkA expression rate	5.04E-08	1.26E-08
$f_{G,ppc}$	ppc expression rate	7.86E-08	8.89E-09
$f_{G,ppsA}$	ppsA expression rate	2.06E-07	1.09E-06
$f_{G,pykF}$	pykF expression rate	5.20E-07	4.59E-08
$f_{D,ACoA}$	Dilution rate of ACoA	6.22E-05	1.06E-04
$f_{D,AKG}$	Dilution rate of AKG	3.56E-05	6.11E-05
$f_{D,cAMP}$	Dilution rate of cAMP	3.56E-05	2.22E-04
$f_{D,FBP}$	Dilution rate of FBP	1.17E-03	1.56E-05
$f_{D,G6P}$	Dilution rate of G6P	3.29E-04	6.50E-05
$f_{D,GLX}$	Dilution rate of GLX	1.78E-12	7.50E-05
$f_{D,ICT}$	Dilution rate of ICT	2.40E-07	8.56E-05
$f_{D,MAL}$	Dilution rate of MAL	6.40E-04	3.69E-04
$f_{D,OAA}$	Dilution rate of OAA	8.89E-06	3.89E-06
$f_{D,PEP}$	Dilution rate of PEP	3.73E-05	3.28E-05
$f_{D,PG3}$	Dilution rate of PG3	1.02E-03	7.50E-05
$f_{D,PYR}$	Dilution rate of PYR	1.60E-04	1.67E-06
$f_{D,AceA}$	Degr.&dilution rate of AceA	9.63E-07	8.61E-06
$f_{D,AceB}$	Degr.&dilution rate of AceB	2.89E-07	2.58E-06
$f_{D,AceK}$	Degr.&dilution rate of AceK	2.89E-08	2.58E-07
$f_{D,Acoa2act}$	Degr.&dilution rate of Acoa2act	0	0
$f_{D,Acs}$	Degr.&dilution rate of Acs	7.53E-09	2.81E-08
$f_{D,Akg2mal}$	Degr.&dilution rate of Akg2mal	2.06E-07	1.75E-07
$f_{D,CAMPdegr}$	Degr.&dilution rate of CAMPdegr	0	0
$f_{D,Cra}$	Degr.&dilution rate of Cra	0	0
$f_{D,CraFBP}$	Degr.&dilution rate of CraFBP	0	0
$f_{D,Crp}$	Degr.&dilution rate of Crp	0	0
$f_{D,CrpcAMP}$	Degr.&dilution rate of CrpcAMP	0	0
$f_{D,Cya}$	Degr.&dilution rate of Cya	0	0
$f_{D,EIIA}$	Degr.&dilution rate of EIIA	0	0
$f_{D,EIIA-P}$	Degr.&dilution rate of EIIA-P	0	0
$f_{D,EIICB}$	Degr.&dilution rate of EIICB	0	0
$f_{D,Emp}$	Degr.&dilution rate of Emp	2.37E-06	8.10E-07
$f_{D,Eno}$	Degr.&dilution rate of Eno	2.37E-06	5.22E-07

continued on the next page ...

... Table S4 continued.

Name of state	Description	Data on glucose	Data on acetate
$f_{D,Fdp}$	Degr.&dilution rate of Fdp	1.56E-08	2.05E-08
$f_{D,GltA}$	Degr.&dilution rate of GltA	6.09E-08	8.45E-08
$f_{D,Icd}$	Degr.&dilution rate of Icd	8.80E-07	2.06E-07
$f_{D,Icd-P}$	Degr.&dilution rate of Icd-P	3.67E-08	6.19E-07
$f_{D,IclR}$	Degr.&dilution rate of IclR	0	0
$f_{D,MaeAB}$	Degr.&dilution rate of MaeAB	2.06E-07	2.84E-07
$f_{D,Mdh}$	Degr.&dilution rate of Mdh	1.02E-07	1.31E-07
$f_{D,PckA}$	Degr.&dilution rate of PckA	7.01E-08	2.34E-07
$f_{D,Pdh}$	Degr.&dilution rate of Pdh	2.08E-07	3.18E-08
$f_{D,PdhR}$	Degr.&dilution rate of PdhR	0	0
$f_{D,PdhRPYR}$	Degr.&dilution rate of PdhRPYR	0	0
$f_{D,PfkA}$	Degr.&dilution rate of PfkA	5.04E-08	1.26E-08
$f_{D,Ppc}$	Degr.&dilution rate of Ppc	7.86E-08	8.89E-09
$f_{D,PpsA}$	Degr.&dilution rate of PpsA	2.06E-07	1.09E-06
$f_{D,PykF}$	Degr.&dilution rate of PykF	5.20E-07	4.59E-08
$f_{BM,ACoA}$	Biomass flux from ACoA	0.658	0.206
$f_{BM,AKG}$	Biomass flux from AKG	0.196	6.11E-02
$f_{BM,G6P}$	Biomass flux from G6P	0.284	8.89E-02
$f_{BM,OAA}$	Biomass flux from OAA	0.320	0.100
$f_{BM,PEP}$	Biomass flux from PEP	8.89E-02	2.78E-02
$f_{BM,PG3}$	Biomass flux from PG3	0.284	8.89E-02
$f_{BM,PYR}$	Biomass flux from PYR	0.498	0.156

2.4 Parameter values

This section contains Table S5, which lists the parameter values determined through application of the divide–and–conquer approach, described in Section 2.1, on the derived data sets, presented in Sections 2.2 and 2.3.

Table S5: Comprehensive list of the parameters **p**, their mechanistic meanings, and their values as determined by the divide–and–conquer approach (see Section 2) on the data presented in Tables S3 and S4..

Parameter	Description	Value
$p_{ENV,M_{ACT}}$	Molar mass of acetate	180.2 $g_{ACT}\,mol^{-1}$
$p_{ENV,M_{GLC}}$	Molar mass of glucose	60 $g_{GLC}\,mol^{-1}$
$p_{ENV,UC}$	Unit conversion	9.5E-07 $g_{DW}\,(\mu[OD])^{-1}$
$p_{AceA,k_{cat}}$	Specific activity	1.03E+04 $\mu mol\,(g_{Prot}\,s)^{-1}$
$p_{AceA,n}$	Number of subunits	4
$p_{AceA,L}$	Allosteric constant	5.01E+04
$p_{AceA,K_{ICT}}$	Affinity constant	0.022 $\mu mol\,g_{DW}{}^{-1}$
$p_{AceA,K_{PEP}}$	Affinity constant	0.055 $\mu mol\,g_{DW}{}^{-1}$
$p_{AceA,K_{PG3}}$	Affinity constant	0.72 $\mu mol\,g_{DW}{}^{-1}$
$p_{AceA,K_{AKG}}$	Affinity constant	0.827 $\mu mol\,g_{DW}{}^{-1}$
$p_{AceB,k_{cat}}$	Specific activity	47.8 $\mu mol\,(g_{Prot}\,s)^{-1}$
$p_{AceB,K_{GLX}}$	Affinity constant	0.95 $\mu mol\,g_{DW}{}^{-1}$
$p_{AceB,K_{ACoA}}$	Affinity constant	0.755 $\mu mol\,g_{DW}{}^{-1}$
$p_{AceB,K_{GLXACoA}}$	Affinity constant	0.719 $\mu mol\,g_{DW}{}^{-1}$
$p_{AceK,k_{cat,ki}}$	Specific activity	3.4E+12 s^{-1}
$p_{AceK,k_{cat,ph}}$	Specific activity	1.7E+09 s^{-1}
$p_{AceK,n}$	Number of subunits	2
$p_{AceK,L}$	Allosteric constant	1.0E+08
$p_{AceK,K_{Icd}}$	Affinity constant	0.043 $g_{Prot}\,g_{DW}{}^{-1}$
$p_{AceK,K_{Icd-P}}$	Affinity constant	0.643 $g_{Prot}\,g_{DW}{}^{-1}$
$p_{AceK,K_{PEP}}$	Affinity constant	0.539 $\mu mol\,g_{DW}{}^{-1}$
$p_{AceK,K_{PYR}}$	Affinity constant	0.038 $\mu mol\,g_{DW}{}^{-1}$
$p_{AceK,K_{OAA}}$	Affinity constant	0.173 $\mu mol\,g_{DW}{}^{-1}$
$p_{AceK,K_{GLX}}$	Affinity constant	0.866 $\mu mol\,g_{DW}{}^{-1}$
$p_{AceK,K_{AKG}}$	Affinity constant	0.82 $\mu mol\,g_{DW}{}^{-1}$
$p_{AceK,K_{PG3}}$	Affinity constant	1.57 $\mu mol\,g_{DW}{}^{-1}$
$p_{AceK,K_{ICT}}$	Affinity constant	0.137 $\mu mol\,g_{DW}{}^{-1}$
$p_{Acoa2act,k_{cat}}$	Specific activity	3079 $\mu mol\,(g_{Prot}\,s)^{-1}$
$p_{Acoa2act,n}$	Number of subunits	2
$p_{Acoa2act,L}$	Allosteric constant	6.39E+05
$p_{Acoa2act,K_{ACoA}}$	Affinity constant	0.022 $\mu mol\,g_{DW}{}^{-1}$

continued on the next page ...

... Table S5 continued.

Parameter	Description	Value
$p_{Acoa2act,K_{PYR}}$	Affinity constant	0.022 $\mu mol\, g_{DW}{}^{-1}$
$p_{Acs,k_{cat}}$	Specific activity	340 $\mu mol\, (g_{Prot}\, s)^{-1}$
$p_{Acs,K_{ACT}}$	Affinity constant	1.0E-03 $g_{ACT}\, l^{-1}$
$p_{Akg2mal,k_{cat}}$	Specific activity	1530 $\mu mol\, (g_{Prot}\, s)^{-1}$
$p_{Akg2mal,K_{AKG}}$	Affinity constant	0.548 $\mu mol\, g_{DW}{}^{-1}$
$p_{CAMPdegr,k_{cat}}$	Specific activity	1 $\mu mol\, (g_{Prot}\, s)^{-1}$
$p_{CAMPdegr,K_{cAMP}}$	Affinity constant	0.1 $\mu mol\, g_{DW}{}^{-1}$
$p_{Cya,k_{cat}}$	Specific activity	993 $\mu mol\, (g_{Prot}\, s)^{-1}$
$p_{Cya,K_{EIIA-P}}$	Affinity constant	1.7E-03 $g_{Prot}\, g_{DW}{}^{-1}$
$p_{Emp,k_{cat,f}}$	Specific activity of forward reaction	1011 $\mu mol\, (g_{Prot}\, s)^{-1}$
$p_{Emp,k_{cat,r}}$	Specific activity of of reverse reaction	857 $\mu mol\, (g_{Prot}\, s)^{-1}$
$p_{Emp,K_{FBP}}$	Affinity constant	5.92 $\mu mol\, g_{DW}{}^{-1}$
$p_{Emp,K_{PG3}}$	Affinity constant	16.6 $\mu mol\, g_{DW}{}^{-1}$
$p_{Eno,k_{cat,f}}$	Specific activity of forward reaction	705 $\mu mol\, (g_{Prot}\, s)^{-1}$
$p_{Eno,k_{cat,r}}$	Specific activity of reverse reaction	530 $\mu mol\, (g_{Prot}\, s)^{-1}$
$p_{Eno,K_{PG3}}$	Affinity constant	4.76 $\mu mol\, g_{DW}{}^{-1}$
$p_{Eno,K_{PEP}}$	Affinity constant	1.11 $\mu mol\, g_{DW}{}^{-1}$
$p_{Fdp,k_{cat}}$	Specific activity	5676 $\mu mol\, (g_{Prot}\, s)^{-1}$
$p_{Fdp,n}$	Number of subunits	4
$p_{Fdp,L}$	Allosteric constant	4.0E+06
$p_{Fdp,K_{FBP}}$	Affinity constant	3.0E-03 $\mu mol\, g_{DW}{}^{-1}$
$p_{Fdp,K_{PEP}}$	Affinity constant	0.3 $\mu mol\, g_{DW}{}^{-1}$
$p_{GltA,k_{cat}}$	Specific activity	1614 $\mu mol\, (g_{Prot}\, s)^{-1}$
$p_{GltA,K_{OAA}}$	Affinity constant	0.029 $\mu mol\, g_{DW}{}^{-1}$
$p_{GltA,K_{ACoA}}$	Affinity constant	0.212 $\mu mol\, g_{DW}{}^{-1}$
$p_{GltA,K_{OAACoA}}$	Affinity constant	0.029 $\mu mol\, g_{DW}{}^{-1}$
$p_{GltA,K_{AKG}}$	Affinity constant	0.63 $\mu mol\, g_{DW}{}^{-1}$
$p_{Icd,k_{cat}}$	Specific activity	695 $\mu mol\, (g_{Prot}\, s)^{-1}$
$p_{Icd,n}$	Number of subunits	2
$p_{Icd,L}$	Allosteric constant	127
$p_{Icd,K_{ICT}}$	Affinity constant	1.6E-04 $\mu mol\, g_{DW}{}^{-1}$
$p_{Icd,K_{PEP}}$	Affinity constant	0.334 $\mu mol\, g_{DW}{}^{-1}$
$p_{MaeAB,k_{cat}}$	Specific activity	1879 $\mu mol\, (g_{Prot}\, s)^{-1}$
$p_{MaeAB,n}$	Number of subunits	1.33
$p_{MaeAB,L}$	Allosteric constant	1.04E+05

continued on the next page ...

... Table S5 continued.

Parameter	Description	Value
$p_{MaeAB,K_{MAL}}$	Affinity constant	6.24E-03 $\mu mol\, g_{DW}{}^{-1}$
$p_{MaeAB,K_{ACoA}}$	Affinity constant	3.64 $\mu mol\, g_{DW}{}^{-1}$
$p_{MaeAB,K_{cAMP}}$	Affinity constant	6.54 $\mu mol\, g_{DW}{}^{-1}$
$p_{Mdh,k_{cat}}$	Specific activity	5437 $\mu mol\, (g_{Prot}\, s)^{-1}$
$p_{Mdh,n}$	Hill coefficient	1.7
$p_{Mdh,K_{MAL}}$	Affinity constant	10.1 $\mu mol\, g_{DW}{}^{-1}$
$p_{PckA,k_{cat}}$	Specific activity	377 $\mu mol\, (g_{Prot}\, s)^{-1}$
$p_{PckA,K_{OAA}}$	Affinity constant	0.184 $\mu mol\, g_{DW}{}^{-1}$
$p_{PckA,K_{PEP}}$	Affinity constant	1000 $\mu mol\, g_{DW}{}^{-1}$
$p_{Pdh,k_{cat}}$	Specific activity	5479 $\mu mol\, (g_{Prot}\, s)^{-1}$
$p_{Pdh,n}$	Number of subunits	2.65
$p_{Pdh,L}$	Allosteric constant	3.4
$p_{Pdh,K_{PYR}}$	Affinity constant	0.128 $\mu mol\, g_{DW}{}^{-1}$
$p_{Pdh,K_{I,PYR}}$	Affinity constant	0.231 $\mu mol\, g_{DW}{}^{-1}$
$p_{Pdh,K_{GLX}}$	Affinity constant	0.218 $\mu mol\, g_{DW}{}^{-1}$
$p_{PfkA,k_{cat}}$	Specific activity	5.39E+05 $\mu mol\, (g_{Prot}\, s)^{-1}$
$p_{PfkA,n}$	Number of subunits	4
$p_{PfkA,L}$	Allosteric constant	9.5E+07
$p_{PfkA,K_{G6P}}$	Affinity constant	0.022 $\mu mol\, g_{DW}{}^{-1}$
$p_{PfkA,K_{PEP}}$	Affinity constant	0.138 $\mu mol\, g_{DW}{}^{-1}$
$p_{Ppc,k_{cat}}$	Specific activity	1.49E+04 $\mu mol\, (g_{Prot}\, s)^{-1}$
$p_{Ppc,n}$	Number of subunits	3
$p_{Ppc,L}$	Allosteric constant	5.2E+06
$p_{Ppc,K_{PEP}}$	Affinity constant	0.048 $\mu mol\, g_{DW}{}^{-1}$
$p_{Ppc,K_{FBP}}$	Affinity constant	0.408 $\mu mol\, g_{DW}{}^{-1}$
$p_{PpsA,k_{cat}}$	Specific activity	1.32 $\mu mol\, (g_{Prot}\, s)^{-1}$
$p_{PpsA,n}$	Number of subunits	2
$p_{PpsA,L}$	Allosteric constant	1.0E-79
$p_{PpsA,K_{PYR}}$	Affinity constant	1.77E-03 $\mu mol\, g_{DW}{}^{-1}$
$p_{PpsA,K_{PEP}}$	Affinity constant	1.0E-03 $\mu mol\, g_{DW}{}^{-1}$
$p_{PykF,k_{cat}}$	Specific activity	1.37E+04 $\mu mol\, (g_{Prot}\, s)^{-1}$
$p_{PykF,n}$	Number of subunits	4
$p_{PykF,L}$	Allosteric constant	1.0E+05
$p_{PykF,K_{PEP}}$	Affinity constant	5 $\mu mol\, g_{DW}{}^{-1}$
$p_{PykF,K_{FBP}}$	Affinity constant	0.413 $\mu mol\, g_{DW}{}^{-1}$
p_{PTS,k_1}	Specific activity	116 $g_{DW}(g_{Prot}\, s)^{-1}$
p_{PTS,km_1}	Specific activity	46.3 $g_{DW}(g_{Prot}\, s)^{-1}$
p_{PTS,k_4}	Specific activity	2520 $\mu mol\, (g_{Prot}\, s)^{-1}$
$p_{PTS,K_{EIIA}}$	Affinity constant	8.5E-03 $g_{Prot}\, g_{DW}{}^{-1}$

continued on the next page ...

... Table S5 continued.

Parameter	Description	Value
$p_{PTS,K_{GLC}}$	Affinity constant	1.2E-03 $g_{GLC}\, l^{-1}$
$p_{Cra,scale}$	Specific activity	100 $g_{Prot}\, (\mu mol\, s)^{-1}$
$p_{Cra,K_{FBP}}$	Affinity constant	1.36 $\mu mol\, {g_{DW}}^{-1}$
$p_{Cra,n}$	Hill coefficient	2
$p_{Crp,scale}$	Specific activity	1.0E+08 $g_{Prot}\, (\mu mol\, s)^{-1}$
$p_{Crp,K_{cAMP}}$	Affinity constant	0.895 $\mu mol\, {g_{DW}}^{-1}$
$p_{Crp,n}$	Hill coefficient	1
$p_{PdhR,scale}$	Specific activity	100 $g_{Prot}\, (\mu mol\, s)^{-1}$
$p_{PdhR,K_{PYR}}$	Affinity constant	0.164 $\mu mol\, {g_{DW}}^{-1}$
$p_{PdhR,n}$	Hill coefficient	1
$p_{aceBAK,aceBfactor}$	Scaling factor	0.3
$p_{aceBAK,aceKfactor}$	Scaling factor	0.03
$p_{aceBAK,k_{cat,IclR}}$	Specific activity	9.3E-04 s^{-1}
$p_{aceBAK,K_{DNA}}$	Affinity constant	2.19 $[AU]\, {g_{DW}}^{-1}$
$p_{aceBAK,DNA}$	DNA concentration	1 $[AU]\, {g_{DW}}^{-1}$
$p_{aceBAK,K_{PYR}}$	Affinity constant	0.897 $\mu mol\, {g_{DW}}^{-1}$
$p_{aceBAK,K_{PYRprime}}$	Affinity constant	3.01E-03 $\mu mol\, {g_{DW}}^{-1}$
$p_{aceBAK,K_{GLX}}$	Affinity constant	4.88E-03 $\mu mol\, {g_{DW}}^{-1}$
$p_{aceBAK,L}$	Allosteric constant	923
$p_{aceBAK,v_{Cra,unbound}}$	Basal expression rate	1.9E-09 $g_{Prot}(g_{DW}\, s)^{-1}$
$p_{aceBAK,v_{Cra,bound}}$	Max. expression rate	2.0E-06 $g_{Prot}(g_{DW}\, s)^{-1}$
$p_{aceBAK,K_{Cra}}$	Affinity constant	3.65E-03 $g_{Prot}\, {g_{DW}}^{-1}$
$p_{aceBAK,v_{Crp,unbound}}$	Max. expression rate	2.0E-08 $g_{Prot}(g_{DW}\, s)^{-1}$
$p_{aceBAK,v_{Crp,bound}}$	Basal expression rate	2.3E-10 $g_{Prot}(g_{DW}\, s)^{-1}$
$p_{aceBAK,K_{Crp}}$	Affinity constant	0.341 $g_{Prot}\, {g_{DW}}^{-1}$
$p_{acs,v_{Crp,unbound}}$	Basal expression rate	0 $g_{Prot}(g_{DW}\, s)^{-1}$
$p_{acs,v_{Crp,bound}}$	Max. expression rate	4.0E-08 $g_{Prot}(g_{DW}\, s)^{-1}$
$p_{acs,n}$	Hill coefficient	2.31
$p_{acs,K_{Crp}}$	Affinity constant	4.7E-03 $g_{Prot}\, {g_{DW}}^{-1}$
$p_{akg2mal,v_{Crp,unbound}}$	Basal expression rate	0 $g_{Prot}(g_{DW}\, s)^{-1}$
$p_{akg2mal,v_{Crp,bound}}$	Max. expression rate	1.4E-06 $g_{Prot}(g_{DW}\, s)^{-1}$
$p_{akg2mal,K_{Crp}}$	Affinity constant	0.091 $g_{Prot}\, {g_{DW}}^{-1}$
$p_{akg2mal,n}$	Hill coefficient	0.74
$p_{emp,v_{Cra,unbound}}$	Max. expression rate	6.1 E-07 $g_{Prot}(g_{DW}\, s)^{-1}$
$p_{emp,v_{Cra,bound}}$	Basal expression rate	0 $g_{Prot}(g_{DW}\, s)^{-1}$
$p_{emp,K_{Cra}}$	Affinity constant	0.09 $g_{Prot}\, {g_{DW}}^{-1}$
$p_{emp,v_{Crp,unbound}}$	Basal expression rate	0 $g_{Prot}(g_{DW}\, s)^{-1}$
$p_{emp,v_{Crp,bound}}$	Max. expression rate	4.7 E-07 $g_{Prot}(g_{DW}\, s)^{-1}$
$p_{emp,K_{Crp}}$	Affinity constant	0.012 $g_{Prot}\, {g_{DW}}^{-1}$

continued on the next page ...

... Table S5 continued.

Parameter	Description	Value
$p_{eno,v_{Cra,unbound}}$	Max. expression rate	6.7 E-07 $g_{Prot}(g_{DW}\, s)^{-1}$
$p_{eno,v_{Cra,bound}}$	Basal expression rate	0 $g_{Prot}(g_{DW}\, s)^{-1}$
$p_{eno,K_{Cra}}$	Affinity constant	0.016 $g_{Prot}\, g_{DW}{}^{-1}$
$p_{fdp,v_{Cra,unbound}}$	Basal expression rate	0 $g_{Prot}(g_{DW}\, s)^{-1}$
$p_{fdp,v_{Cra,bound}}$	Max. expression rate	2.1E-08 $g_{Prot}(g_{DW}\, s)^{-1}$
$p_{fdp,K_{Cra}}$	Affinity constant	1.18E-03 $g_{Prot}\, g_{DW}{}^{-1}$
$p_{gltA,v_{Crp,unbound}}$	Basal expression rate	0 $g_{Prot}(g_{DW}\, s)^{-1}$
$p_{gltA,v_{Crp,bound}}$	Max. expression rate	6.5E-07 $g_{Prot}(g_{DW}\, s)^{-1}$
$p_{gltA,K_{Crp}}$	Affinity constant	0.04 $g_{Prot}\, g_{DW}{}^{-1}$
$p_{gltA,n}$	Hill coefficient	1.07
$p_{icd,v_{Cra,unbound}}$	Basal expression rate	1.1E-07 $g_{Prot}(g_{DW}\, s)^{-1}$
$p_{icd,v_{Cra,bound}}$	Max. expression rate	8.5E-07$g_{Prot}(g_{DW}\, s)^{-1}$
$p_{icd,K_{Cra}}$	Affinity constant	1.17E-03 $g_{Prot}\, g_{DW}{}^{-1}$
$p_{mdh,v_{Crp,unbound}}$	Basal expression rate	0 $g_{Prot}(g_{DW}\, s)^{-1}$
$p_{mdh,v_{Crp,bound}}$	Max. expression rate	1.3 E-06 $g_{Prot}(g_{DW}\, s)^{-1}$
$p_{mdh,K_{Crp}}$	Affinity constant	0.06 $g_{Prot}\, g_{DW}{}^{-1}$
$p_{pckA,v_{Cra,unbound}}$	Basal expression rate	0 $g_{Prot}(g_{DW}\, s)^{-1}$
$p_{pckA,v_{Cra,bound}}$	Max. expression rate	3.7 E-07 $g_{Prot}(g_{DW}\, s)^{-1}$
$p_{pckA,K_{Cra}}$	Affinity constant	5.35E-03 $g_{Prot}\, g_{DW}{}^{-1}$
$p_{pdh,v_{PdhR,unbound}}$	Max. expression rate	7.7 E-08 $g_{Prot}(g_{DW}\, s)^{-1}$
$p_{pdh,v_{PdhR,bound}}$	Basal expression rate	2.8 E-10 $g_{Prot}(g_{DW}\, s)^{-1}$
$p_{pdh,K_{PdhR}}$	Affinity constant	3.4E-03 $g_{Prot}\, g_{DW}{}^{-1}$
$p_{pfkA,v_{Cra,unbound}}$	Max. expression rate	1.4 E-06 $g_{Prot}(g_{DW}\, s)^{-1}$
$p_{pfkA,v_{Cra,bound}}$	Basal expression rate	1.1 E-08 $g_{Prot}(g_{DW}\, s)^{-1}$
$p_{pfkA,K_{Cra}}$	Affinity constant	6.3E-07 $g_{Prot}\, g_{DW}{}^{-1}$
$p_{ppsA,v_{Cra,unbound}}$	Basal expression rate	0 $g_{Prot}(g_{DW}\, s)^{-1}$
$p_{ppsA,v_{Cra,bound}}$	Max. expression rate	3.3E-06 $g_{Prot}(g_{DW}\, s)^{-1}$
$p_{ppsA,K_{Cra}}$	Affinity constant	0.017 $g_{Prot}\, g_{DW}{}^{-1}$
$p_{pykF,v_{Cra,unbound}}$	Max. expression rate	1.6 E-07 $g_{Prot}(g_{DW}\, s)^{-1}$
$p_{pykF,v_{Cra,bound}}$	Basal expression rate	8.8 E-10 $g_{Prot}(g_{DW}\, s)^{-1}$
$p_{pykF,K_{Cra}}$	Affinity constant	2.3E-03 $g_{Prot}\, g_{DW}{}^{-1}$
$p_{D,k_{degr}}$	Universal protein degradation rate	2.8E-05 s^{-1}
$p_{BM,k_{expr}}$	Gene expression rate constant	2.0E+04 s
$p_{BM,\mu_{ACT}}$	Growth rate on acetate	5.6E-05 s^{-1}
$p_{BM,\mu_{GLC}}$	Growth rate on glucose	1.8E-04 s^{-1}
$p_{BM,GLC_{ACoA}}$	1st order rate constant	1.88 s^{-1}
$p_{BM,GLC_{AKG}}$	1st order rate constant	0.978 s^{-1}

continued on the next page ...

... Table S5 continued.

Parameter	Description	Value
$p_{BM,GLC_{G6P}}$	1st order rate constant	0.154 s^{-1}
$p_{BM,GLC_{OAA}}$	1st order rate constant	6.4 s^{-1}
$p_{BM,GLC_{PEP}}$	1st order rate constant	0.423 s^{-1}
$p_{BM,GLC_{PG3}}$	1st order rate constant	0.049 s^{-1}
$p_{BM,GLC_{PYR}}$	1st order rate constant	0.553 s^{-1}
$p_{BM,ACT_{ACoA}}$	1st order rate constant	0.108 s^{-1}
$p_{BM,ACT_{AKG}}$	1st order rate constant	0.056 s^{-1}
$p_{BM,ACT_{G6P}}$	1st order rate constant	0.076 s^{-1}
$p_{BM,ACT_{OAA}}$	1st order rate constant	1.43 s^{-1}
$p_{BM,ACT_{PEP}}$	1st order rate constant	0.047 s^{-1}
$p_{BM,ACT_{PG3}}$	1st order rate constant	0.066 s^{-1}
$p_{BM,ACT_{PYR}}$	1st order rate constant	5.185 s^{-1}

3 Sensitivity analysis

The sensitivities of each of the two reproduced steady states with respect to small parameter perturbations were approximated through

$$S_{i,j} = \frac{\Delta x_i / x_i}{\Delta p_j / p_j} \approx \frac{(x_i^+ - x_i^-)/x_i}{(1.01\,p_j - 0.99\,p_j)/p_j} = \frac{x_i^+ - x_i^-}{0.02\,x_i} \quad ,$$

with x_i the nominal steady state value and x_i^+ and x_i^- the values resulting from a 1% increase or decrease, respectively, of the parameter value p_j. As a heatmap of the resulting 47x193 sensitivity matrix S is too large for convenient inspection, we reduced the size of S by grouping the sensitivities of those parameters that appear in the same rate equation f_k. For this grouping, we used the size-independent overall variability

$$S_{i,k} = \frac{1}{n_k} \sum_{j \,|\, p_j \in f_k} S_{i,j}^2$$

as sensitivity statistics, with n_k the number of parameters appearing in f_k. The results of these local sensitivity analyses, one for each of the two steady states, are plotted in Figure S2.

This figure reveals that in general, protein and metabolite concentrations respond differently to parameter perturbations. Protein concentrations are most significantly affected by perturbations of the parameters describing their gene's expression but are rather marginally affected by other parameter perturbations, causing the red diagonal line of high protein sensitivities in Figure S2. In contrast, the sensitivities of the metabolite concentrations do not form such a line. Therefore, contrary to what might have been expected, the sensitivities of metabolite concentrations to parameter variations of their topological enzyme neighbors and to more distant perturbation are about the same. We suspect that this property of the metabolites' sensitivities is due to the model's densely interconnected enzymatic regulation.

A further observation is that sensitivities that are high on glucose are often low on acetate and vice versa, probably because many reactions are very active in one condition but much less so in the other.

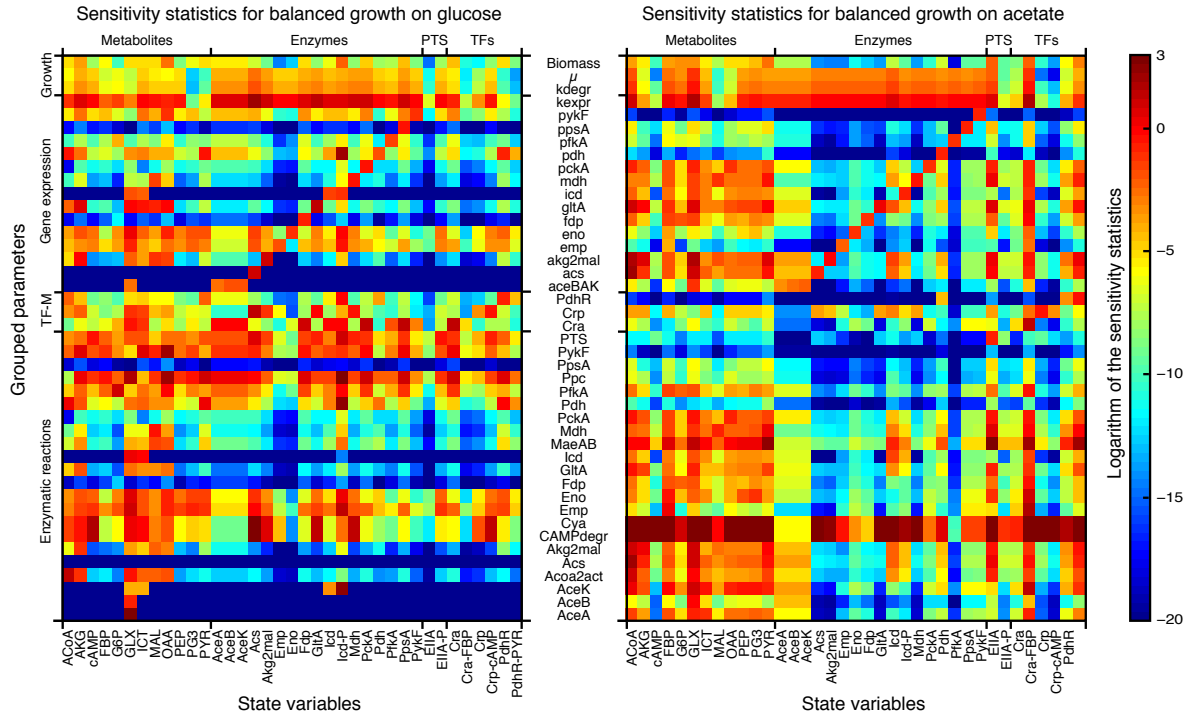

Figure S2: Sensitivity statistics of the steady states with respect to 1% parameter perturbations. The used statistics condenses the sensitivities of all parameters appearing in the same rate equation to a single value.

4 Simulation results

In this section, we present the simulated time profiles of the intracellular metabolites (Figure S3), enzymes (Figure S4), rates (Figures S5 and S6), the phosphorylation state of the proteins EIIA and Icd, and the TF activities (Figure S7). Figure S8 contains a subset of these time profiles to illustrate the connection between the available extracellular carbon sources, the concentrations of the intracellular signal metabolites, and the activities of their target TFs. These time profiles are based on the parameter vector listed in Table S5. Note that due to the uncertainty in the parameter values, the ambiguity in the selection of rate laws, and possible effects of not modeled cellular regulations, i.e. those ensuring the here omitted energy, cofactor etc. balances, onto the simulated trajectories, these profiles cannot be considered a quantitatively accurate reproduction of the *in vivo* time profiles. Instead, these profiles are meant to demonstrate that with the chosen parameters, (i) all compound concentrations and rates approach the proper steady state levels and (ii) remain within physiologically reasonable bounds throughout the transitions.

An aspect worth noting is the spiking of some metabolite concentrations following environmental changes. Such fast changes in metabolite levels have already been observed in time-resolved metabolomics experiments (Bettenbrock et al, 2006; Chassagnole et al, 2002). In some cases such as OAA, these spikes might be an artifact of the modeling, caused by the fast change of the used first order rate constants upon a change in environmental conditions (see Section 1.9). In other cases, however, the spikes arise from the interplay of mechanistically modeled interactions. For instance, PEP and PYR spike because they are coupled to glucose uptake via the PTS system. These spikes propagate through the system: G6P's small upward spike following the change from glucose to acetate is a consequence of the large upward PEP spike quickly inhibiting the G6P–consuming reaction (in the model, PfkA) while quickly activating the G6P–producing (back-)reaction from FBP (in the model, Fdp); G6P's steady state convergence after that small, initial spike is slow because G6P is immediately formed by the uptake of glucose but needs many reaction steps to be synthesized from acetate.

Another aspect worth mentioning is that the *duration* of the transition period between balanced growth on either substrate is primarily determined by the growth rates and is therefore robust to the inherent uncertainty in the model. The reason for this is that the speed of steady state convergence is given by the slowest significant rates of the model, which are the enzyme dilution rates due to growth. This observation suggests that with μ the growth rate on the condition adapting to, a lower bound (that neglects active protein degradation) for the transcriptional adaptation time of bacteria could be quantified, e.g. in the form of a 'minimal half-adaptation time' $T_{1/2} = \mu^{-1} ln(2)$.

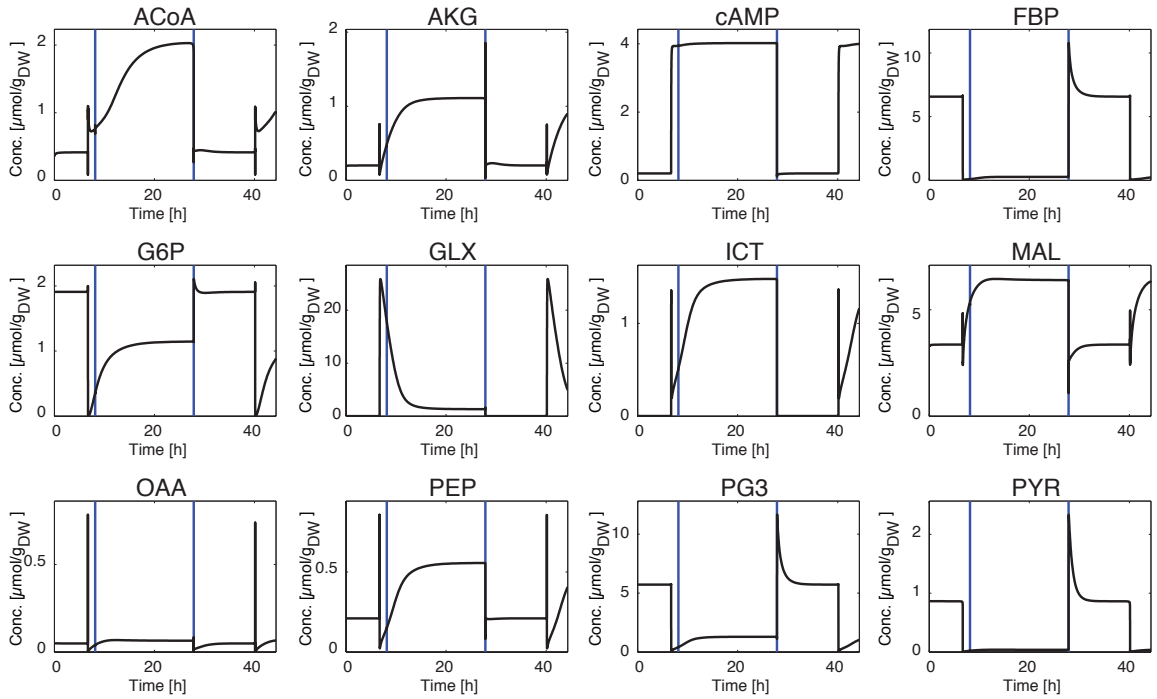

Figure S3: Simulated intracellular metabolite concentrations. The vertical blue lines indicate the time instants of external changes to the available carbon sources (see Figure S8 or main paper). The concentrations approach the measured steady state values listed in Table S3.

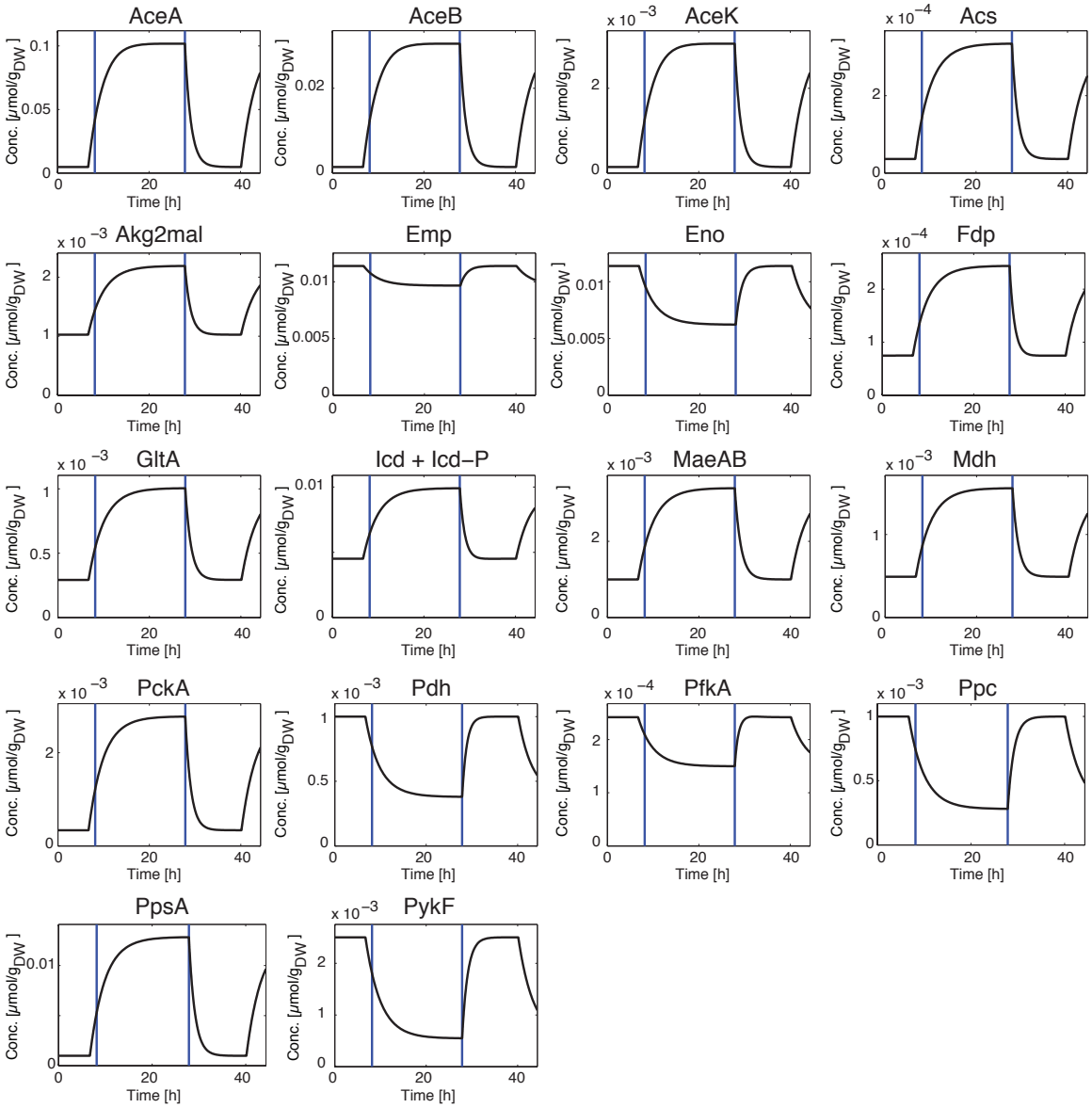

Figure S4: Simulated enzyme concentrations. The vertical blue lines indicate the time instants of external changes to the available carbon sources (see Figure S8 or main paper). The concentrations approach the measured steady state values listed in Table S3.

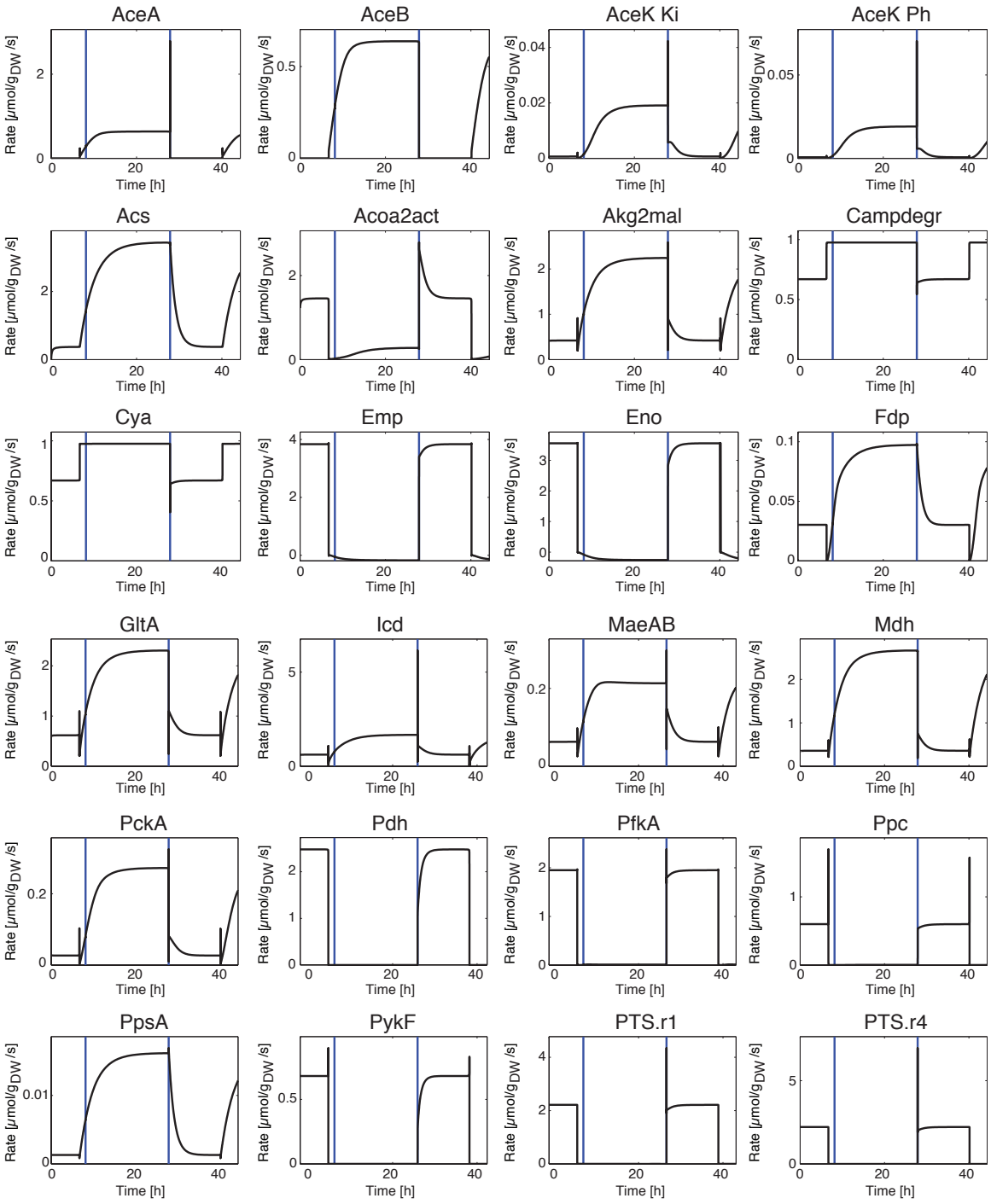

Figure S5: Simulated enzymatic reaction rates. The vertical blue lines indicate the time instants of external changes to the available carbon sources (see Figure S8 or main paper). The rates approach the measured steady state values listed in Table S4.

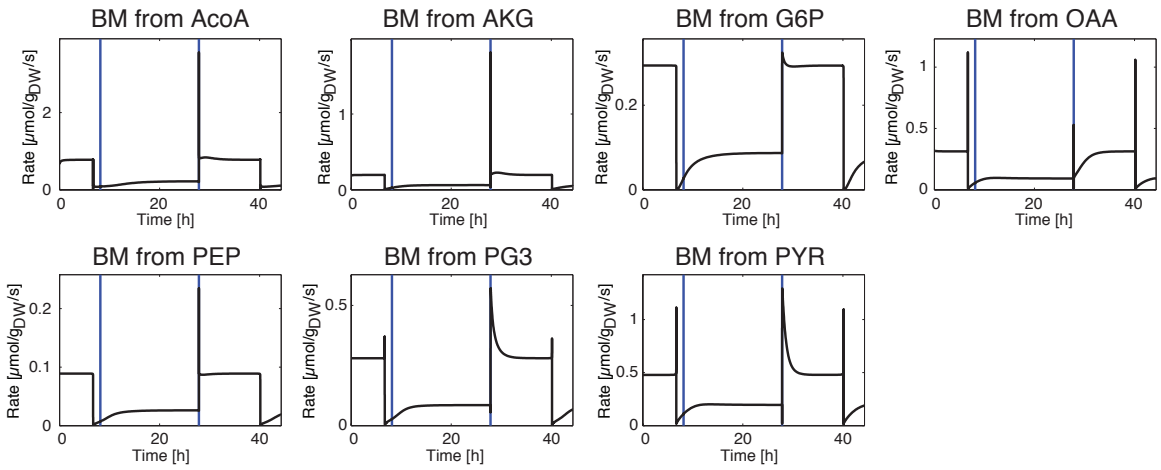

Figure S6: Simulated biomass reaction rates. The vertical blue lines indicate the time instants of external changes to the available carbon sources (see Figure S8 or main paper). The rates approach the measured steady state values listed in Table S4.

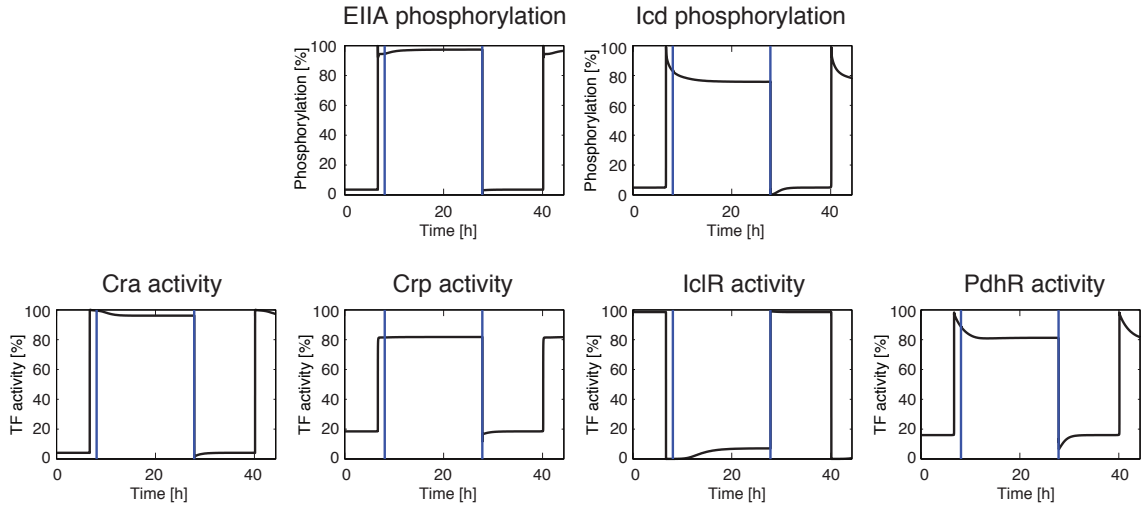

Figure S7: Simulated phosphorylation states of the proteins EIIA and Icd, and simulated TF activities. The vertical blue lines indicate the time instants of external changes to the available carbon sources (see Figure S8 or main paper). The phosphorylation states and TF activities approach the measured steady state values listed in Table S3.

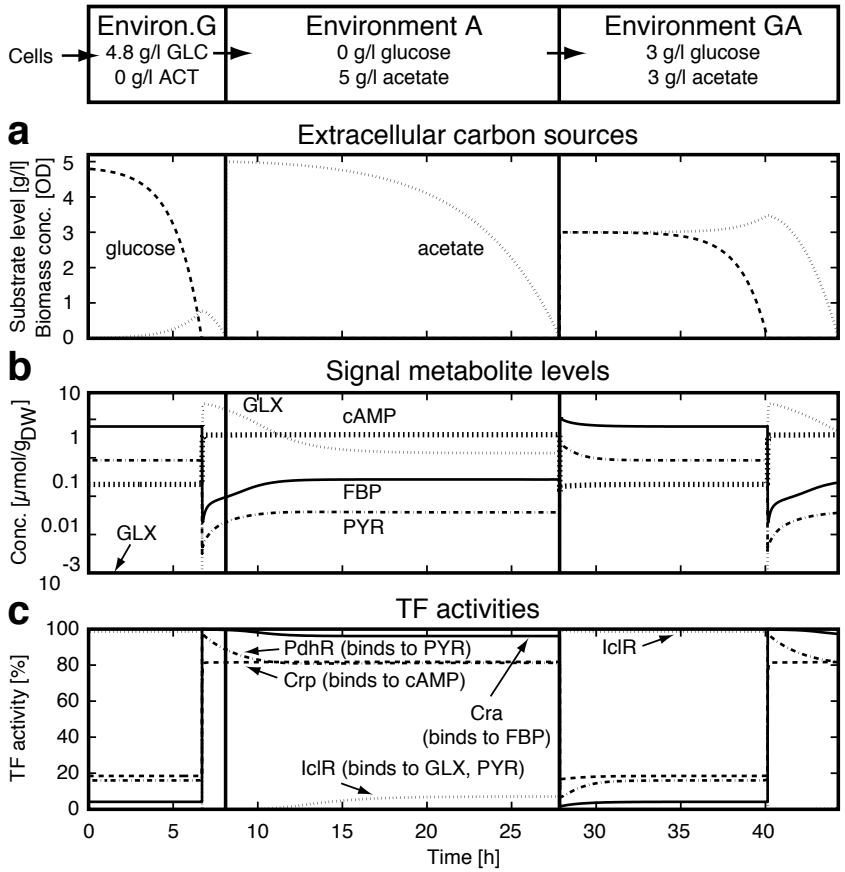

Figure S8: The concentrations of the four signal metabolites and the activities of their four target TFs respond to the presence of extracellular carbon sources. **a**, Levels of extracellular carbon sources. **b**, Levels of intracellular signal metabolites. **c**, Activities of the signal metabolites' target TFs.

5 Contributions of individual interactions to the overall response

The model presented in the previous sections of this Supplementary Information offers a consistent explanation of how a multitude of known molecular interactions fit into a coherent systems picture. In the model, the interactions work together like gear wheels that mesh with one another to adapt central metabolism between growth on the glycolytic substrate glucose and the gluconeogenic substrate acetate, as demonstrated in the main paper.

A particularly interesting question is which of the modeled interactions are necessary to perform the adaptation, and which are not engaged in the adaptation. In general, the adaptation rests on the collective action of many interactions such that the successive removal of these interactions leads to gradually worse adaptations (the term 'worse' here means an increase in the distance between the measured steady state and the simulated steady state assumed after the carbon source change).

Naturally, some interactions have a more important contribution to the overall response than others. A quantification of the contributions of individual interactions to the overall response depends on the chosen rate laws and parameters, which are to some degree uncertain. Therefore, we here discuss the *qualitative* importance of individual interactions *to the proper functioning of the distributed sensing and adjustment mechanism*. A few interactions are essential to this adaptation, most interactions play a 'supporting' role such that their removal can be to some degree compensated by the collective action of the remaining interactions, and some interactions are present in the model but are not engaged in the adaptation mechanism, as discussed below.

The contributions of individual interactions to the overall response operate on two time scales, the fast time scale of enzyme regulations and the slow time scale of transcriptional regulations.

Correlation of flux signalling-metabolite levels with metabolic fluxes To ensure that the levels of flux-signalling metabolites indicate the metabolic flux through a pathway, the kinetics of the enzymes surrounding these metabolites must establish a correlation between the metabolite levels and the fluxes. These correlations are established through either of the general motifs *pathway usage* or *flux direction*, as presented in the main paper. In molecular detail, the distinct and thus informative levels of the flux–signalling metabolites are established, through the two general motifs, as follows.

- To establish a low level of cAMP on glucose, the phosphorylated form of the PTS protein EIIA, EIIA-P, which activates cAMP synthesis via the enzyme Cya, must be sufficiently low. In turn, a low level of EIIA-P arises if the affinity constant of the PTS's glucose uptake reaction for the PTS protein EIIA, $p_{PTS,K_{EIIA}}$, is low enough.

- To establish a high level of FBP on glucose, the affinity constant for FBP of the FBP–consuming enzyme 'Emp', $p_{Emp,K_{FBP}}$, must be sufficiently high.

- To establish a high level of PYR on glucose, the affinity constant for PYR of the PYR–consuming enzyme Pdh, $p_{Pdh,K_{PYR}}$, must be sufficiently high.

- To establish a low level of GLX on glucose, the glyoxylate shunt may not be induced. At the ICT branch point, metabolic flux is directed to the lower TCA if Icd's phosphorylated form, Icd-P, is sufficiently low. The phosphorylation state of Icd is highly regulated by the AceK kinase and phosphatase reactions. Essentially, the levels of the regulating metabolites AKG, GLX, ICT, OAA, PEP, PG3 and PYR and AceK's affinity constants for these effectors must be balanced such that for these effectors' steady state levels on glucose, the phosphatase reaction dominates to such an extent that Icd-P levels are negligible. Furthermore, to favor the lower TCA route over the glyoxylate shunt route, the affinity constant for ICT of the enzyme AceA ($p_{AceA,K_{ICT}}$), which catalyzes the glyoxylate shunt's first reaction, must be markedly higher than the affinity constant for ICT of the enzyme Icd ($p_{Icd,K_{ICT}}$), which catalyzes the lower TCA cycle's first reaction.

- To establish a high level of cAMP on acetate, the phosphorylated form of the PTS protein EIIA, EIIA-P, which activates cAMP synthesis via the enzyme Cya, must be sufficiently high. Absent glucose uptake, the phosphorylation state of the PTS protein EIIA equilibrates with the PEP/PYR ratio. Therefore, a high enough level of EIIA-P follows when the PEP/PYR ratio is sufficiently high, which translates into a sufficiently high PEP level and a sufficiently low PYR level. As glucose uptake converts PEP to PYR, inactivity of this reaction due to glucose absence necessarily increases the PEP/PYR ratio. A sufficiently high affinity constant for PEP of the PEP–consuming enzyme Eno, $p_{Eno,K_{PEP}}$, and a sufficiently low affinity constant for PYR of the PYR–consuming enzyme PpsA, $p_{PpsA,K_{PYR}}$, can further contribute to a high PEP/PYR ratio on acetate.

- To establish a low level of FBP on acetate, the affinity constant for FBP of the FBP–consuming enzyme Fdp, $p_{Fdp,K_{FBP}}$, must be sufficiently low. A second contribution to a low level of FBP on acetate arises if Fdp's affinity constant for its activator PEP, $p_{Fdp,K_{PEP}}$, is low enough, and this activation is strong enough (the allosteric constant $p_{Fdp,L}$ is high enough) — then, the relatively high level of Fdp's activator PEP on acetate (due to an inactive, PEP–consuming PTS reaction and a sufficiently high affinity constant for PEP of the PEP–consuming enzyme Eno, $p_{Eno,K_{PEP}}$) activates Fdp sufficiently so that this enzyme can realize the required gluconeogenic flux even with a low level of its substrate FBP.

- To establish a low level of PYR on acetate, the affinity constant for PYR of the PYR–consuming enzyme PpsA, $p_{PpsA,K_{PYR}}$, must be sufficiently low.

- To establish a high level of GLX on acetate, the glyoxylate shunt must be induced, and the affinity constant of the GLX–consuming reaction AceB, $p_{AceB,K_{GLX}}$, must be sufficiently high. To induce the glyoxylate shunt on acetate, the Icd reaction must be sufficiently inactivated through a high level of Icd-P, which results from a proper balancing of AceK's affinity constants, as noted above.

Note that the proposed distributed sensing mechanism can work as long as the flux-signalling metabolite levels contain sufficient flux information. Therefore, the above mentioned parameters may vary as long as they ensure that the flux-signalling metabolite levels can still indicate flux. Similarly, not–modelled regulations such as those that fulfill energy, cofactor, pH and proton balances may modulate the system dynamics as long as these modulations do not compromise the correlation between the flux-signalling metabolite levels and the flux through these metabolites.

Binding of flux-signalling metabolites to TFs For the operation of the proposed distributed sensing mechanism, it is essential that the information present in the levels of the flux-signalling metabolites is propagated into informative TF activities. Therefore, the distinct levels of the flux-signalling metabolites on glucose and acetate must lead to distinct levels of the target TFs' activities. This propagation must be enabled by the affinity constants of the TFs for their effectors, e.g. $p_{Cra,K_{FBP}}$, which must therefore lie in the range of the effector concentrations. The best propagation of distinct metabolite levels into distinct TF activities is achieved if these affinity constants lie in between the steady state metabolite levels on glucose and acetate. However, the sensing mechanism can work as long as the propagation of the flux information from metabolite levels into TF activities occurs to a sufficient degree, despite possible impacts of not-modelled regulations as well as uncertainties in the model structure and parameter values.

Coupling of flux-signalling metabolite levels The coupling of flux-signalling metabolites through network topology is explained in the main paper. As long as the metabolite levels are coupled to a sufficient degree, the transcriptional adjustments of the four TFs produce a concerted response of the overall system.

Enzymatic regulations contributing to proper network operation During model development, we learned that the following enzymatic regulations, although not engaged in the sensing mechanism, do perform important regulatory adjustments and are thus important for proper network operation.

- **Inhibition of PfkA by PEP and activation of Fdp by PEP** The enzymes PfkA and Fdp catalyze the same reaction step in opposing directions; during growth on glucose, the PfkA reaction dominates whereas during growth on acetate, the Fdp reaction dominates. On the transcriptional level, PfkA production is inhibited by Cra and Fdp production is activated by Cra. Hence, during steady state growth on either glucose or acetate, one of these two enzymes is expressed while the other is repressed, and therefore the 'correct' reaction direction is favored. However, in early stages of the transition from one of the steady states to the other, the reaction must already operate in the 'correct' direction although the enzyme levels have not yet been adjusted and thus still favor the 'wrong' reaction direction. To enable the necessary, rapid reversal of carbon flux, PfkA and Fdp must be antagonistically regulated not only on the slow time scale of transcriptional regulations but also on the fast time scale of enzymatic regulations. Furthermore, the

antagonistic enzymatic regulation supports the antagonistic transcriptional regulation also during steady state growth, as it further suppresses the 'wrong' reaction direction and thereby helps to prevent futile cycling between G6P and FBP.

- **Inhibition of Pdh by GLX** During growth on glucose, the Pdh reaction is very active as the primary route to supply the TCA cycle with carbon derived from glucose. However, during growth on acetate, it is very important that the Pdh reaction is suppressed in order to prevent the carbon derived from acetate, which has been converted from acetyl-CoA to pyruvate, to cycle back to acetyl-CoA, which is acetate's point of entry into central metabolism. We found that to successfully adapt from glucose to acetate, it is crucial that already in early stages of the adaptation, the carbon derived from the TCA cycle enters the gluconeogenesis pathway and does *not* cycle back to acetyl-CoA. To divert the carbon flux coming from malate to PEP and not to acetyl-CoA, the acetyl-CoA producing Pdh reaction is inhibited by GLX, which assumes a high level on acetate but not on glucose. Intriguingly, this regulation couples the induction of the glyoxylate shunt to the repression of the Pdh reaction, which makes sense given the functional role of these two pathways.

- **Inhibition of MaeAB by acetyl-CoA and cAMP** The levels of MaeAB's inhibitors acetyl-CoA and cAMP are high on acetate but low on glucose. These enzymatic regulations thus seem to oppose the experimentally verified (Fuhrer et al, 2005; Zhao et al, 2004) usage of the MaeAB reaction, which is used on acetate but not on glucose. However, our model suggests that this apparent contradiction only concerns steady state growth, and that these enzymatic regulations play important roles *during the transition* from glucose to acetate. As noted above, we find that for successful adaptations from glucose to acetate, it is crucial that the cell employs enzymatic regulation to divert its carbon flux to the gluconeogenesis pathway and prevent it from cycling back to acetyl-CoA via the Pdh reaction. In addition to regulating the PYR branch point, as noted above, the cell can also regulate the upstream MAL branch point and divert carbon flux to PEP via OAA, and not to PEP via PYR from which it may cycle back to acetyl-CoA. The inhibition of MaeAB by acetyl-CoA, which is the product of the Pdh reaction, is particularly interesting and functionally very meaningful: If the Pdh reaction from PYR to acetyl-CoA is active on acetate, then there is too much influx into the PYR branch point to direct all of the carbon to the gluconeogenesis pathway. When this occurs, then the level of acetyl-CoA rises and feeds back onto the regulation of the MAL branch point. Because of the negative feedback regulation of MaeAB by acetyl-CoA, the MAL branch point is adjusted such that the alternative route to PEP via OAA is favored. Note that the activity of the negative enzymatic feedback regulation of acetyl-CoA onto the MaeAB reaction can be seen in Figure S5: Flux through MaeAB reaches its steady state rate on acetate faster than e.g. the PckA and PpsA rates do — once the MaeAB flux has increased to a certain degree, the enzymatic feedback kicks in, prevents the otherwise occurring

further increase in the rate, and stabilizes the MaeAB flux at a rate that does not 'overload' the PYR branch point. In our opinion, this insight is a formidable example how kinetic studies can suggest the functions of apparently contradictory molecular regulations through analyzing transient, dynamic behavior.

- **Activation of Acoa2act by PYR** As pyruvate levels are high when glucose is present, this enzymatic regulation ensures that significant acetate uptake occurs only in the absence of glucose. In the presence of glucose, co–metabolization of acetate is discouraged.

- **Activation of PykF and Ppc by FBP** As noted above, PEP is an important effector for the sensing mechanism. The level of PEP is high on acetate but low on glucose. On acetate, a high PEP level is ensured by an inactive, PEP–consuming PTS reaction and by a sufficiently high affinity constant for PEP of the PEP–consuming enzyme Eno, $p_{Eno,K_{PEP}}$. On glucose, a low PEP level is ensured by the PEP–consuming PTS reaction being active, and by the activation of the two PEP–consuming enzymes PykF and Ppc by FBP (which has a high level on glucose but not on acetate, see above).

Enzymatic regulations opposing the proposed adaptation mechanism Some enzymatic regulations oppose the functioning of the proposed distributed sensing and adjustment mechanism. The here proposed mechanism functions if these regulations are weak enough, which is very likely given that these regulation oppose the experimentally verified behavior at least in steady state, as noted below. We speculate that these regulations have a function that is not covered by the here presented model (from a modular viewpoint on cellular regulation, these regulations would belong to other regulatory subsystems). These regulations could be eliminated from the model without affecting its capability for successful adaptations. A list of these regulations follows.

- **Inhibition of PckA and PpsA by PEP** The high level of the inhibitor PEP on acetate oppose the experimentally verified (Fuhrer et al, 2005; Zhao et al, 2004) usage of the PckA and PpsA reactions, which are needed on acetate but not on glucose.

- **Inhibition of Pdh by PYR** The high level of PYR on glucose and the experimentally verified strong usage of the Pdh reaction on glucose (Fuhrer et al, 2005) oppose the inhibition of Pdh by PYR.

- **Inhibition of AceA by AKG and PEP** The high levels of AKG and PEP on acetate and the experimentally verified usage of the glyoxylate shunt on acetate (Zhao et al, 2004) oppose the inhibition of AceA, which catalyzes the first reaction of the glyoxylate shunt, by AKG and PEP.

Transcriptional regulations Because the model topology has been assembled around four TFs, the transcriptional adjustment of the model's enzyme levels is regulated by

these TFs alone. However, the contributions of each of these four TFs to the successful adaptation of the overall system to carbon source changes differ markedly.

The TFs Cra and Crp regulate the production of many enzymes in central metabolism and as such play an essential role in the adaptation. If either one of these two TFs is removed, the adaptations are not successful. The transcriptional regulations of IclR and PdhR, however, are much more specific than those of Cra and Crp; thus, their deletion is easier to compensate.

In the model and in real *E. coli* cells, the only operon regulated by the TF IclR is the glyoxylate shunt operon, *aceBAK*. As this operon is co–regulated by Cra (and Crp, which, however, regulates the operon in the 'wrong' direction, for whatever reason), the in silico cell could compensate a deletion of IclR through the transcriptional regulation of Cra. Therefore, the in silico cell does not require the TF IclR to adapt between growth on glucose and acetate. However, the induction of the glyoxylate shunt is *in vivo* very likely more selective than in the model: The glyoxylate shunt is required for growth on acetate but not for growth on other gluconeogenic carbon sources such as succinate, malate or fumarate. We speculate that the *in vivo* function of IclR is the selective induction of the glyxoylate shunt for growth on acetate but not on other gluconeogenic carbon sources — an aspect not included in the *in silico cell*, for which acetate is the sole gluconeogenic carbon source.

In the model and in real *E. coli* cells, the only enzyme regulated by the TF PdhR is Pdh. For a successful adaptation from glucose to acetate, a suppression of the Pdh reaction is crucial. This suppression is to a large extent accomplished through enzymatic regulations, as discussed above. These enzymatic regulations are supported through the transcriptional regulation of PdhR. Without PdhR, the enzymatic regulation of Pdh activity still ensure a successful adaptation, yet the reached steady state on acetate exhibits a decerased gluconeogenic flux (the acetate steady state exhibits an elevated level of the enzyme Pdh; consequentially, at the PYR branch point, the flux to acetyl-CoA is increased and therefore the flux to PEP, the entry point of gluconeogenesis, is decreased). Therefore, PdhR is not essential for the modelled adaptation but rather plays a supportive role. This result predicts a lower–than–wild–type growth rate of the *in vivo* strain lacking Pdh on acetate.

References

Bettenbrock K, Fischer S, Kremling A, Jahreis K, Sauter T, Gilles, ED (2006) A quantitative approach to catabolite repression in *Escherichia coli. J Biol Chem.* **281**:2578-2584.

Yagil G, Yagil E (1971) On the relation between effector concentration and the rate of induced enzyme synthesis. *Biophys J.* **11**:11-27.

Chung T, Resnik E, Stueland C, LaPorte, DC (1993) Relative expression of the products of glyoxylate bypass operon: contributions of transcription and translation. *J Bacteriol.* **175**:4572-4575.

Ishihama Y, Schmidt T, Rappsilber J, Mann M, Hartl FU, Kerner MJ, Frishman D (2008) Protein abundance profiling of the *Escherichia coli* cytosol. *BMC Genomics* **9**:102.

Tao H, Bausch C, Richmond C, Blattner FR, Conway T (1999) Functional genomics: expression analysis of *Escherichia coli* growing on minimal and rich media. *J Bacteriol.* **181**:6425-6440.

Chassagnole C, Noisommit-Rizzi N, Schmid JW, Mauch K, Reuss M (2002) Dynamic modeling of the central carbon metabolism of *Escherichia coli. Biotechnol Bioeng.* **79**:53-73.

Kümmel A, Panke S, Heinemann M (2006) Putative regulatory sites unraveled by network-embedded thermodynamic analysis of metabolome data. *Mol Syst Biol.* **2**:2006.0034.

Epstein W, Rothman-Denes LB, Hesse J. (1975) Adenosine 3':5'-cyclic monophosphate as mediator of catabolite repression in *Escherichia coli. Proc Natl Acad Sci U S A.* **72**:2300-2304.

el-Mansi EM, Nimmo HG, Holms WH (1986) Pyruvate metabolism and the phosphorylation state of isocitrate dehydrogenase in *Escherichia coli. J Gen Microbiol.* **132**:797-806.

Crasnier-Mednansky M, Park MC, Studley WK, Saier MH Jr. (1997) Cra-mediated regulation of *Escherichia coli* adenylate cyclase. *Microbiology* **143**:785-792.

Peng L, Arauzo-Bravo MJ, Shimizu K (2004) Metabolic flux analysis for a *ppc* mutant *Escherichia coli* based on 13C-labelling experiments together with enzyme activity assays and intracellular metabolite measurements. *FEMS Microbiol Lett.* **235**:17-23.

Rahman M, Hasan MR, Oba T, Shimizu K. (2006) Effect of *rpoS* gene knockout on the metabolism of *Escherichia coli* during exponential growth phase and early stationary phase based on gene expressions, enzyme activities and intracellular metabolite concentrations. *Biotechnol Bioeng.* **94**:585-595.

Anderson WB, Schneider AB, Emmer M, Perlman RL, Pastan I (1971) Purification of and properties of the cyclic adenosine 3':5'-monophosphate receptor protein which mediates 3':5'-monophosphate dependent gene transcription in *Escherichia coli*. *J Biol Chem.* **246**:5929-5937.

Oh MK, Liao JC (2000) Gene expression profiling by DNA microarrays and metabolic fluxes in *Escherichia coli*. *Biotechnol Prog.* **16**:278-286.

Walsh K, Koshland DE Jr (1984) Determination of flux through the branch point of two metabolic cycles. The tricarboxylic acid cycle and the glyoxylate shunt. *J Biol Chem.* **259**:9646-9654.

Fuhrer T, Fischer E, Sauer U (2005) Experimental identification and quantification of glucose metabolism in seven bacterial species. *J Bacteriol.* **187**:1581-1590.

Zhao J, Baba T, Mori H, Shimizu K. (2004) Effect of *zwf* gene knockout on the metabolism of *Escherichia coli* grown on glucose or acetate. *Metab Eng.* **6**:164-174.